Open access • Journal Article • DOI:10.1007/BF01579914

Phenomenology of Σ+→pℓ+ℓ− and the structure of the weak non-leptonic Hamiltonian — Source link

L. Bergström, R. Safadi, P. Singer

Institutions: Stockholm University, Technion – Israel Institute of Technology, CERN

Published on: 01 Jun 1988 - European Physical Journal C (Springer-Verlag)

CERN-TH.4728/87

PHENOMENOLOGY OF $\Sigma^+ \to p\ell^+\ell^-$ AND THE STRUCTURE OF THE WEAK NON-LEPTONIC HAMILTONIAN

Lars Bergström
Department of Theoretical Physics, University of Stockholm
S-11346 Stockholm, Sweden

Rafi' Safadi
Department of Physics, Technion-Israel Institute of Technology
Haifa, Israel

and

Paul Singer*)
CERN - Geneva

ABSTRACT

The problem of the radiative non-leptonic weak baryon decays is reviewed in light of the new experimental findings. With the aim of exploring the structure of the weak non-leptonic Hamiltonian, we present a detailed phenomenological analysis of $\Sigma^+ \to p\ell^+\ell^-$ transitions. Lower and upper limits for rates derivable with standard physics are determined as $\Gamma(\Sigma^+ \to pe^+e^-)/\Gamma(\Sigma^+ \to p\gamma) \geq 7.2\times10^{-3}$ and $1/1210 \lesssim \Gamma(\Sigma^+ \to p\mu^+\mu^-)/\Gamma(\Sigma^+ \to pe^+e^-) \lesssim 1/120$. From existing data on $\Sigma^+ \to pe^+e^-$ we obtain limits on the values of the charge radius form factors $|c_1/b_1| \lesssim 5$; $|c_2/b_1| \lesssim 10$, where the magnetic form factor is given by the $\Sigma^+ \to p\gamma$ decay as $b_1(0) = 6.9 \pm 0.9$ MeV. The short distance contribution of the QCD corrected single quark $s \to d\gamma$ transition is shown not to play a dominant role in these decays.

---

*) On leave from Technion-Israel Institute of Technology, Haifa.

CERN-TH.4728/87
May 1987

1. - INTRODUCTION

The weak radiative decays of baryons have attracted the continuous interest of theorists during the last two decades[1)-16)]. This ongoing attention is related in an obvious way to the gradual evolving of the theoretical techniques; these lead to the successive treatment of these decays from symmetry concepts[1),2)] and pole models as well as more sophisticated models on the hadronic level[3),7)-9)] to the modern approach of the effective Hamiltonian of quarks and gluons, which is based on the Weinberg-Salam theory of electroweak interactions to which QCD corrections are administered[4)-6),9)-16)]. The fact that photon emission is simpler to treat theoretically than the corresponding pion emission of non-leptonic decays, has kept alive the hope that these decays will provide the needed insight into the structure of the weak non-leptonic Hamiltonian. This hope has not materialized yet. In fact, the recent surge of interest in these decays[6)-16)] has been fuelled to a large extent by the unsolved puzzle of the large negative asymmetry parameter observed in $\Sigma^+ \to p\gamma$ decay[17)], $\alpha(\Sigma^+ \to p\gamma) \simeq -0.8$. This value deviates considerably from the expectation of a vanishing parity-violating amplitude as required by exact SU(3) flavour symmetry[1)].

While the parity-violating term in the transition $\Sigma^+ \to p\gamma$ vanishes by virtue of U-spin symmetry[1),2)], relaxing the SU(3) flavour symmetry condition does not lead in an obvious way to a large and negative asymmetry parameter. On the contrary, it has been known for some time[4),5)] that in a simple quark picture, one is led by general considerations to a parity-violating amplitude of relative size $(m_s-m_d)/(m_s+m_d)$, giving an asymmetry parameter which is positive and large if current quark masses are used.

An important step in the treatment of the $B_1 \to B_2\gamma$ decays has been taken through the analysis of Gilman and Wise[10)]. These authors (GW) start with the assumption that all the $B_1 \to B_2\gamma$ weak decays in the 56-multiplet of SU(6) are due to a single-quark transition and parametrize this amplitude by two parameters a and b which represent the effective parity-conserving and parity-violating components respectively. In order to calculate the $B_1 \to B_2\gamma$ decays, GW take the hadrons to be described by SU(6) quark model wave functions and assume that the overlap of the hadronic wave functions is common to all transitions. If the parameters a, b are thus determined from the $\Sigma^+ \to p\gamma$ decay, one may then proceed to calculate the branching ratios (B_{GW}^{th}) for $\Lambda \to n\gamma$, $\Xi^0 \to \Sigma^0\gamma$,

$\Xi^0 \to \Lambda\gamma$, $\Xi^- \to \Sigma^-\gamma$, $\Omega^- \to \Xi^-\gamma$ and $\Omega^- \to \Xi^{-*}\gamma$. It turns out that some of these come out quite large, of the order of 10^{-2}, which is already in conflict with existing measurements and upper limits. For example, with the assumptions of GW one obtains $B^{th}_{GW}(\Lambda \to n\gamma) = 2.2\times10^{-2}$ while a recent measurement[18] gives $B^{exp}(\Lambda \to n\gamma) = (1.02\pm0.33)\times10^{-3}$ and likewise $B^{th}_{GW}(\Xi^0 \to \Lambda\gamma) = 4\times10^{-3}$ versus $B^{exp}(\Xi^0 \to \Lambda\gamma) = (1.1\pm0.2)\times10^{-3}$ [19a] and $B^{th}_{GW}(\Xi^- \to \Sigma^-\gamma) = 1.1\times10^{-2}$ versus $B^{exp}(\Xi^- \to \Sigma^-\gamma) = (2.3\pm1.0)\times10^{-4}$ [19b]. There is also an experimental upper limit on the Ω^- radiative decay of $B^{exp}(\Omega^- \to \Xi^-\gamma) < 2.2\times10^{-3}$ [20] versus the GW prediction of $B^{th}_{GW}(\Omega^- \to \Xi^-\gamma) = 4.1\times10^{-2}$. The assumption that all these decays are given by the single-quark transition $s \to d\gamma$ is obviously untenable and the quark model analysis should be extended to include also two-quark and three-quark transitions, as exhibited in Fig. 1. Nevertheless, one should remember that in some of these decays, like $\Omega^- \to \Xi^-\gamma$, in which the transitions depicted in Figs. 1b and 1c cannot proceed by the standard weak Hamiltonian because of the quark content of the baryons, the $s \to d\gamma$ may still provide the dominant mechanism[16].

There are several papers[9),11),12)] in which the quark model analysis has been extended to include the two-quark and three-quark transitions. Although there are similarities between these papers, there are also basic differences and we shall refer to the work of Lo[12] as the reference for the application of the standard model to the $\Sigma^+ \to p\gamma$ problem. In this relativistic quark calculation the amplitude for $\Sigma^+ \to p\gamma$ is represented by the sum of the three diagrams of Fig. 1 resulting from the operator product $J^{\mu}_{EM}(x)J^{\nu}_{\Delta S=1}(y)J^{\sigma}_{\Delta S=0}(z)$. The corrections due to soft and hard gluons are included via the MIT bag model for the baryonic states and by the use of the QCD corrected Hamiltonian[21] for the two-quark $\to$ two-quark strangeness changing transition. Lo finds the one-quark transition (Fig. 1a) to be much smaller than the two-quark one (Fig. 1b) and the contribution from Fig. 1c to vanish to the order of the calculation. A negative asymmetry parameter $\alpha(\Sigma^+ \to p\gamma) = -0.154$ is then obtained[12] from the dominant two-quark transition. This figure, though smaller in absolute value than the observed one, has at least the correct sign. However, Lo neglects in his calculation the QCD corrections to the single-quark transition $s \to d\gamma$ which are known to be sizeable for the magnetic part of the transition[5),6),13)], the only one appearing in the decay with real photons. When the QCD corrections are consistently included for all contributing diagrams, an asymmetry parameter of $\alpha(\Sigma^+ \to p\gamma) = -0.22$ is obtained[16], while the rate of $\Sigma^+ \to p\gamma$ is still dominated by the two-quark transition. It should also be mentioned that a certain equivalence has been established[9),12)] between the short distance approach[9),12)] and that

baryon pole model which emphasizes[8),9)] the role of intermediate negative parity baryon resonances in obtaining the negative asymmetry parameter.

The most recent experimental results[18),19a)] are providing now rates for some additional weak radiative modes, $\Lambda^0 \to n\gamma$ and $\Xi^0 \to \Lambda^0\gamma$ which also entertain contributions from two-quark transitions. When these new data are compared with the models which tried to account for several of the radiative $B' \to B\gamma$ modes[7)-11)], one discovers that none is able to reproduce all the experimental figures[18)-20)]. Hence, one is left essentially with the approach of the standard model as used by Lo[12)], which however has not passed yet the test of the extension to other modes, and in any case it gives $\alpha(\Sigma^+ \to p\gamma)$ too small[12),16)]. Also, there is the singular attempt of Gaillard, Li and Rudaz[15)] who investigated the possiblity that the $sd\gamma g$ vertex is responsible for the baryonic weak radiative transition, on the assumption that a sizeable gluonic component resides in the baryonic wave function. Although the $sd\gamma g$ operator can give rise to parity-conserving and parity-violating amplitudes of opposite sign, it appears that its contribution to the observed width of $\Sigma^+ \to p\gamma$ is too small to be of dominant role in the actual decay[15)].

An exception to the above remarks is provided by the more exotic $\Omega^- \to \Xi^-(\Xi^{*-})\gamma$ and $\Xi^- \to \Sigma^-\gamma$ decays to which the two-quark → two-quark transitions cannot contribute; for these modes, single-quark transitions[16)], penguin diagrams[14)] and long-distance contributions[13)] are relevant. For the Ω^- radiative decay, the single-quark transition is expected[16),22)] to dominate, but the existing experimental upper limit[20)] does not allow yet to distinguish among the various models. On the other hand, the recent measurement[19b)] of the rate of $\Xi^- \to \Sigma\gamma$ agrees well with the calculation[13)] of the long range contribution to this decay, as expected theoretically from a comparison[22)] of the various contributions to this mode.

In the processes discussed so far, it is the magnetic part of the radiative transition which is tested. In general, the radiative $B' \to B\gamma$ vertex has two independent components, a magnetic part and a charge radius part (see next section for details), the latter vanishing for transitions to real photons. In view of the present impasse of the problem, and for its own intrinsic interest, it should be very valuable to test both components of the radiative transition in the same process. Various models would give different predictions for these two parts, and their measurement in a specific process could help to achieve the much sought after insight into the structure of the QCD corrected weak Hamiltonian[22)]. For example, in the free quark model, the $sd\gamma$ amplitude (with

virtual photon) has a negligible magnetic part as compared to the charged radius one[23)-26)]. However, when QCD corrections are included[6),21),27)], the magnetic term is increased substantially while the charge radius term essentially retains its size though it changes sign.

In this paper we consider the possibility of using the $\Sigma^+ \to p\ell^+\ell^-$ decays as a tool for the investigation of models for the non-leptonic weak radiative decays. To this end, we present here the phenomenology of this decay and we analyze the sensitivity of various measurable quantities to the relative size and sign of the independent components of the radiative amplitude. While it is too early to confront predictions of models in any detail, we show that some limits on the charge radius amplitudes are already derivable from existing data. Also, the single-quark transitions are calculated and found to play a minor role in these decays. In the second section, we present definitions and the various distributions in the $\Sigma^+ \to p\ell^+\ell^-$ decay, the third section contains a numerical analysis and the last section is the discussion of our results.

2. - THE AMPLITUDE AND DECAY DISTRIBUTIONS OF $\Sigma^+ \to p\ell^+\ell^-$

Let us denote the decay amplitude for the processes $\Sigma \to pe^+e^-$, $p\mu^+\mu^-$ by M. Using the notation defined[28)] in Fig. 2, one has

$$M = -ie\,G\,M^{\mu}\,\ell_{\mu} \tag{1}$$

where ℓ_μ is the product of the photon propagator and the leptonic current matrix element

$$\ell_\mu = \frac{i}{q^2}(-ie)\,\bar{u}(p_{\ell^-})\,\gamma_\mu\,v(p_{\ell^+}) \tag{2a}$$

and

$$M_\mu = \bar{u}(p)\,\Gamma_\mu\,u(p_\Sigma)\,. \tag{2b}$$

For the hadronic matrix element M_μ we define an effective vertex function Γ_μ whose most general form, as dictated[29),30)] by Lorentz invariance and the assumption that the Σ^+, p satisfy the free particle Dirac equation, is

$$\Gamma^{\mu} = (a_1 + a_2\gamma_5)\,\gamma^{\mu} + (b_1 + b_2\gamma_5)\left(\frac{i}{2}\right)^{-1}\sigma^{\mu\nu}q^{\nu} + (c_1 + c_2\gamma_5)\,q^{\mu}\,. \tag{3}$$

The strength eG of the effective vertex and the form factors $a_1(q^2)$, $a_2(q^2)$, $b_1(q^2)$, $b_2(q^2)$, $c_1(q^2)$, $c_2(q^2)$ contain the combined effects of the electroweak and strong interactions. From the definition of the decay amplitude (1), it is obvious that b_1, b_2, c_1, c_2 have dimensions of mass and a_1, a_2 have dimensions of $(\text{mass})^2$.

It is still necessary to impose electromagnetic gauge invariance, which restricts Γ_μ to fulfil

$$\bar{u}(p)\, q_\mu \Gamma^\mu u(p_\Sigma) = 0 \quad . \tag{4}$$

Using again the Dirac equation for Σ^+ and p, this translates into relations between a_1, c_1 and a_2,c_2:

$$a_1(q^2) = -\frac{q^2}{m_\Sigma - m_p} c_1(q^2); \quad a_2(q^2) = -\frac{q^2}{m_\Sigma + m_p} c_2(q^2) \tag{5}$$

The third term in (3) does not contribute in the actual Dalitz decay ($m_{\ell^+} = m_{\ell^-}$).

For a real photon ($q^2 = 0$, $\varepsilon^{(\gamma)} \cdot q = 0$) and assuming no singular behaviour for $c_1(q^2)$, $c_2(q^2)$, only the mid-term of (3) contributes to the decay amplitude $\Sigma^+ \to p\gamma$. The measurement of the rate and asymmetry of $\Sigma^+ \to p\gamma$ is relevant to the determination of $b_1(0)$ and $b_2(0)$. Using (3) for the decay to a real photon, one obtains for the decay rate Γ and for the asymmetry parameter $\alpha(\Sigma^+ \to p\gamma)$,

$$\frac{d\Gamma(\Sigma^+ \to p\gamma)}{d(\cos\theta)} = 8\alpha G^2 |\vec{q}|^3 \left(|b_1|^2 + |b_2|^2\right)\left[1 + \frac{2\,\mathrm{Re}(b_1 b_2^*)}{|b_1|^2 + |b_2|^2}\cos\theta\right] \tag{6a}$$

where θ is the angle between the polarization vector of Σ^+ and the direction of the proton momentum and $|\vec{q}| = (M_\Sigma^2 - M_p^2)/2M_\Sigma$. Then,

$$\Gamma(\Sigma^+ \to p\gamma) = 16\alpha G^2 \left(|b_1|^2 + |b_2|^2\right) |\vec{q}|^3, \tag{6b}$$

$$\alpha(\Sigma^+ \to p\gamma) = \frac{2\,\mathrm{Re}(b_1 b_2^*)}{|b_1|^2 + |b_2|^2} \quad . \tag{6c}$$

The particle data values for these quantities are[31)]

$$B.R.^{(exp)}(\Sigma^+ \to p\gamma) = (1.22 \pm 0.10) \times 10^{-3} \qquad (7a)$$

which gives

$$\Gamma^{(exp)}(\Sigma^+ \to p\gamma) = (1.01 \pm 0.08) \times 10^{-8}\ eV \qquad (7b)$$

and

$$\alpha^{(exp)}(\Sigma^+ \to p\gamma) = -0.72 \pm 0.29 \ . \qquad (7c)$$

The last figure does not include the KEK experiment which reported[32] a preliminary figure of $\alpha(\Sigma^+ \to p\gamma) = -0.85 \pm 0.013 \pm 0.05$.

Assuming b_1, b_2 are relatively real which is supported by the existing models [e.g., Refs. 11) and 13)], Eqs. (6) and (7) lead to

$$b_2(0)/b_1(0) = -0.42 \pm 0.24\ ;\ |b_1(0)| = 6.9 \pm 0.9\ MeV. \qquad (8)$$

In order to calculate the leptonic decays, it is convenient to perform a Gordon decomposition on (2b) which leads to a redefinition of the vertex function (3) such that $\bar{u}(p)\Gamma_\mu u(p_\Sigma) \to \bar{u}(p)\Gamma'_\mu u(p_\Sigma)$ [remember, the $(c_1+c_2\gamma_5)q_\mu$ term does not contribute in the leptonic decay] where

$$\Gamma'^{\mu} = a\gamma^\mu + b\gamma_5\gamma^\mu + c p_\Sigma^\mu + d\gamma_5 p_\Sigma^\mu \qquad (9)$$

with

$$\begin{aligned} a &\equiv a_1 + 2b_1(m_\Sigma + m_p)\ ;\quad c \equiv -4b_1 \\ b &\equiv a_2 + 2b_2(m_\Sigma - m_p)\ ;\quad d \equiv -4b_2 \end{aligned} \qquad (10)$$

and we made use of $q^\mu \ell_\mu = 0$ for the processes under consideration.

We proceed firstly to calculate the decay distribution in the Σ^+ rest frame. To this end, let us introduce two Lorentz invariant kinematic variables

$$s = q^2 \quad ; \quad t = p_\Sigma \cdot p_{\ell^+} \ . \qquad (11)$$

Following the usual technique[28], one arrives at

$$\frac{d\Gamma(\Sigma^+ \to p\ell^+\ell^-)}{ds} = \frac{(\alpha G)^2}{\pi m_\Sigma^3} \int_{t_{min}}^{t_{max}} \frac{dt}{s^2} \left[\beta(\Delta_+\Delta_- + s - 2t)t + \left(\delta - \frac{\beta m_\Sigma^2 s}{2}\right)\right] \tag{12}$$

where

$$\beta \equiv 2\left[|a|^2 + |b|^2 + Re(ac^*)\Delta_+ + Re(bd^*)\Delta_-\right] + |c|^2 M_+^2 + |d|^2 M_-^2 \tag{13a}$$

$$\delta \equiv (s + 2m_\ell^2)(|a|^2 M_-^2 + |b|^2 M_+^2) \tag{13b}$$

$$M_-^2 \equiv p\cdot p_\Sigma - m_p m_\Sigma \;;\; \Delta_- \equiv m_\Sigma - m_p \tag{13c}$$

$$M_+^2 \equiv p\cdot p_\Sigma + m_p m_\Sigma \;;\; \Delta_+ \equiv m_\Sigma + m_p .$$

The limits of integration are

$$t_{\substack{max\\min}} = \frac{s + \Delta_+\Delta_-}{4} \pm \frac{\lambda^{1/2}(m_\Sigma^2, m_p^2, s)}{4}\left(1 - \frac{4m_\ell^2}{s}\right)^{1/2} \tag{13d}$$

with

$$\lambda = m_\Sigma^4 + m_p^4 + s^2 - 2m_\Sigma^2 m_p^2 - 2m_\Sigma^2 s - 2m_p^2 s . \tag{13e}$$

The lepton invariant mass distribution, after integrating over t in (12), may be given in closed form as

$$\frac{d\Gamma(\Sigma^+ \to p\ell^+\ell^-)}{ds} = \frac{(\alpha G)^2 \beta_\ell \lambda^{1/2}}{2\pi m_\Sigma^3 s^2}\left(1 + \frac{2m_\ell^2}{s}\right)\left[\frac{\beta\lambda}{12} + s(|a|^2 M_-^2 + |b|^2 M_+^2)\right] \tag{14a}$$

where

$$\beta_\ell \equiv \left(1 - \frac{4m_e^2}{s}\right)^{1/2} \quad . \tag{14b}$$

In the numerical analysis presented in the next section, we shall be interested to exhibit the originally defined form factors as given in (3), so as to be able to separate between the magnetic transition expressed via b_1, b_2 on which there is knowledge from the $\Sigma^+ \to p\gamma$ decay, and the a_1, a_2, c_1, c_2 form factors which appear only in the Dalitz decay. We reinstate these coupling in (14a) by use of (10) and divide $d\Gamma(\Sigma^+ \to p\ell^+\ell^-)$ to the total rate for $\Sigma^+ \to p\gamma$, thus obtaining

$$\begin{aligned}
\frac{1}{\Gamma(\Sigma^+\to p\gamma)}\cdot\frac{d\Gamma(\Sigma^+\to p\ell^+\ell^-)}{ds} &= \frac{\alpha}{2\pi}\cdot\frac{(s+2m_\ell^2)\lambda^{1/2}\beta_\ell}{(m_\Sigma^2-m_p^2)^3 s^2(|b_1|^2+|b_2|^2)} \\
&\cdot\Big\{(|b_1|^2+|b_2|^2)\Big[\Delta_+^2\Delta_-^2 - \frac{\lambda}{3} - s(m_\Sigma^2+m_p^2)\Big] \\
&- (|b_1|^2-|b_2|^2)\,2m_\Sigma m_p s + \Big(\frac{|c_1|^2}{\Delta_-^2}+\frac{|c_2|^2}{\Delta_+^2}\Big)\Big[\frac{\lambda s}{12} \\
&+ \frac{s^2}{4}(m_\Sigma^2+m_p^2-s)\Big] - \frac{1}{2}\Big(\frac{|c_1|^2}{\Delta_-^2}-\frac{|c_2|^2}{\Delta_+^2}\Big)s^2 m_\Sigma m_p \\
&- \mathrm{Re}(b_1c_1^*)\frac{s\Delta_+(\Delta_-^2-s)}{\Delta_-} - \mathrm{Re}(b_2c_2^*)\frac{s\Delta_-(\Delta_+^2-s)}{\Delta_+}\Big\}.
\end{aligned} \tag{15}$$

In this expression we have replaced a_1, a_2 by c_1, c_2 using (5) and M_+, M_- by Δ_+, Δ_- using

$$M_+^2 = (\Delta_+^2 - s)/2 \quad ; \quad M_-^2 = (\Delta_-^2 - s)/2 \quad . \tag{16}$$

If one is interested to express this distribution in terms of the momentum $|\vec{p}| \equiv p$ of the recoiling proton, the appropriate expression is

$$\frac{d\Gamma(\Sigma^+\to p\ell^+\ell^-)}{dp} = \frac{2m_\Sigma p}{(p^2+m_p^2)^{1/2}}\cdot\frac{d\Gamma(\Sigma^+\to p\ell^+\ell^-)}{ds} \tag{17}$$

where on the right-hand side of (17) one should replace λ and s as follows:

$$\lambda(m_\Sigma^2, m_p^2, s) = 4 m_\Sigma^2 p \; ; \; s = m_\Sigma^2 + m_p^2 - 2m_\Sigma (p^2 + m_p^2)^{1/2} \quad (18)$$

Turning now to angular asymmetries in decay, we consider the decay of polarized Σ^+ for which we take a polarization vector in the positive direction of the z axis. We choose a covariant polarization vector $n^\mu = (0,\hat{n})$ in the rest system, $\hat{n}\cdot\hat{n} = 1$. The decay kinematics will be expressed in terms of three variables s, t [Eq. (11)] and θ, where θ is the angle between the proton momentum and the polarization vector of Σ^+, $\cos\theta = (\hat{p}\cdot\hat{n}) = z$, $\hat{p}$ being a unit vector in the direction of $\vec{p}$. Our choice of kinematics is resemblant, though not identical, to the analysis previously performed[33] for the kinematically similar decay $\Sigma^0 \to \Lambda e^+ e^-$. We express the angular distribution so as to exhibit the angular asymmetries of the proton and of the antilepton with respect to the Σ^+ polarization:

$$\frac{d\Gamma(\Sigma^+ \to p\ell^+\ell^-)}{ds\,dt\,dz} = F(s,t)\left[1 + V(s,t)\hat{p}\cdot\hat{n} + W(s,t)\hat{p}_{\ell^+}\cdot\hat{n}\right] \quad (19)$$

The angle θ_+ between the polarization vector of Σ^+ and the antilepton momentum, $\cos\theta_+ = \hat{p}_{\ell^+}\cdot\hat{n}$, is expressible in terms of s, t and z[34]. We find

$$F(s,t) = \frac{(\alpha G)^2}{2\pi m_\Sigma^3 s^2}\left[\beta(\Delta_+\Delta_- + s - 2t)t + \left(\delta - \frac{\beta m_\Sigma^2 s}{2}\right)\right], \quad (20)$$

$$V(s,t) = \frac{\lambda^{1/2}}{m_\Sigma}\Big\{m_\Sigma \mathrm{Re}(ab^*)(s+2m_\ell^2) - [\mathrm{Re}(bc^*) + \mathrm{Re}(ad^*) + m_\Sigma \mathrm{Re}(cd^*)]\left[(\Delta_+\Delta_- + s - 2t)t - \frac{m_\Sigma^2 s}{2}\right] \quad (21)$$

$$- t\left(2m_\Sigma \mathrm{Re}(ab^*) + M_+^2 \mathrm{Re}(bc^*) + M_-^2 \mathrm{Re}(ad^*)\right)\Big\}$$

$$\cdot\left[\beta(\Delta_+\Delta_- + s - 2t)t + \left(\delta - \frac{\beta m_\Sigma^2 s}{2}\right)\right]^{-1},$$

$$W(s,t) = \frac{(t^2 - m_\Sigma^2 m_\ell^2)^{1/2}}{m_\Sigma} \Big[2 m_\Sigma \, Re(ab^*) + M_+^2 \, Re(bc^*) + M_-^2 \, Re(ad^*) \Big] \cdot (\Delta_+ \Delta_- + s - 4t) \cdot \Big[\beta (\Delta_+ \Delta_- + s - 2t) t + \Big(\delta - \frac{\beta m_\Sigma^2 s}{2} \Big) \Big]^{-1} , \tag{22}$$

in which we used $2m_\Sigma (n \cdot p) = -\lambda^{\frac{1}{2}} \hat{p} \cdot \hat{n}$ and $m_\Sigma (n \cdot p_{\ell^+}) = -(t^2 - m_\Sigma^2 m_\ell^2)^{\frac{1}{2}} \hat{p}_{\ell^+} \cdot \hat{n}$. Arriving at the expressions (19) to (22), we have neglected terms proportional to $\hat{n} \cdot (\hat{p} \times \hat{p}_{\ell^+})$ which vanish if the amplitudes are relatively real, which we assume.

3.- NUMERICAL RESULTS

In order to simplify the analysis, we assume that in the range of s one is concerned with in the $\Sigma^+ \to p\ell^+\ell^-$ decay, the form factors b_1, b_2, c_1, c_2 are real and constant for all practical purpose. The a_1, a_2 form factors have then the s-dependence given by (5). The reality assumption, as already mentioned, is certainly supported by model calculations [see, e.g., Refs. 10)-13)]. As to the s-variation, a reasonable estimate is obtained by assuming a model which is known to work well for the small q^2 values involved here, like vector meson dominance. For $\Sigma^+ \to pe^+e^-$ where the distribution is peaked very closely to s_{min} around $s \simeq 2$ MeV^2, there is no problem at all, but even for $\Sigma^+ \to p\mu^+\mu^-$ where the distribution peaks around $s \simeq (220 \text{ MeV})^2$, the assumption of vector meson dominance for the form factor induces changes which are at most 10-15%. Thus, one may safely assume constancy for b_1, b_2, c_1, c_2 especially in a first attempt analysis which we are addressing here.

We begin by considering the integrated partial decay rates of $\Sigma^+ \to pe^+e^-$, $\Sigma^+ \to p\mu^+\mu^-$. As it will become obvious from our analysis, the latter is a very sensitive probe to the magnitude of the charge radius form factors. We integrate (15) between $s_{min} = (2m_\ell)^2$ -- the configuration when the two leptons have equal three-momenta, and $s_{max} = (m_\Sigma - m_P)^2$ -- the configuration with the proton at rest, and we replace the constants dependent on m_Σ, m_P, m_e, m_μ by their numerical values[31]. Then,

$$\frac{\Gamma(\Sigma^+ \to p e^+ e^-)}{\Gamma(\Sigma^+ \to p\gamma)} = \left\{ 7.72\times10^{-3}\left[1+\left(\frac{b_2}{b_1}\right)^2\right] - 3.82\times10^{-4}\left[1 - \left(\frac{b_2}{b_1}\right)^2\right] + 3.90\times10^{-5}\left(\frac{c_1}{b_1}\right)^2 + 1.60\times10^{-6}\left(\frac{c_2}{b_1}\right)^2 - 5.45\times10^{-5}\left(\frac{c_1}{b_1}\right) - 9.07\times10^{-5}\left(\frac{b_2}{b_1}\right)\left(\frac{c_2}{b_1}\right)\right\}\left[1+\left(\frac{b_2}{b_1}\right)^2\right]^{-1}, \tag{23}$$

$$\frac{\Gamma(\Sigma^+ \to p \mu^+ \mu^-)}{\Gamma(\Sigma^+ \to p\gamma)} = \left\{ 3.67\times10^{-5}\left[1+\left(\frac{b_2}{b_1}\right)^2\right] - 2.93\times10^{-5}\left[1 - \left(\frac{b_2}{b_1}\right)^2\right] + 7.76\times10^{-7}\left(\frac{c_1}{b_1}\right)^2 + 1.84\times10^{-7}\left(\frac{c_2}{b_1}\right)^2 - 1.05\times10^{-6}\left(\frac{c_1}{b_1}\right) - 6.93\times10^{-6}\left(\frac{b_2}{b_1}\right)\left(\frac{c_2}{b_1}\right)\right\}\left[1+\left(\frac{b_2}{b_1}\right)^2\right]^{-1}. \tag{24}$$

There is one previous calculation by Lyagin and Ginzburg[30] in which these partial decay rates are estimated for the hypothetical case $c_1 = c_2 = 0$, $b_1 = b_2$ [the present knowledge from $\Sigma^+ \to p\gamma$ implies $b_1 \approx -2b_2$, see (8) and the accompanying discussion]. Using their Eq. (10) one finds $\Gamma(\Sigma^+ \to pe^+e^-)/\Gamma(\Sigma^+ \to p\gamma) \approx 1/180$, while the correct figure for this case (i.e., for $c_1 = c_2 = 0$, $b_1 = b_2$) from (23) is $\approx 1/130$. However, fortuitously, Lyagin and Ginzburg used in their calculation only the first term of an expansion, which happens to give the correct value of 1/130 for the particular choice of constants mentioned. Their expression for $\Gamma(\Sigma^+ \to p\mu^+\mu^-)$ is apparently in error since it leads to a value for $\Gamma(\Sigma^+ \to pe^+e^-)/\Gamma(\Sigma^+ \to p\mu^+\mu^-)$ which is off by an order of magnitude.

In Tables 1 and 2 we give the ratios $\Gamma(\Sigma^+ \to p\gamma)/\Gamma(\Sigma^+ \to pe^+e^-)$ and $\Gamma(\Sigma^+ \to pe^+e^-)/\Gamma(\Sigma^+ \to p\mu^+\mu^-)$ respectively for different values of c_1/b_1, c_2/b_1 which are varied between 0 and ±50. The tables are constructed so as to emphasize at which values sizeable changes in these ratios are occurring, compared to the values obtained when $c_1 = c_2 = 0$. In these tables, we used $b_2/b_1 = -0.42$ (8) which corresponds to $\alpha(\Sigma^+ \to p\gamma) = -0.72$[31]. Since the value of

$\alpha(\Sigma^+ \to p\gamma)$ has a very large experimental uncertainty, we checked the sensitivity of $\Gamma(\Sigma^+ \to p\ell^+\ell^-)/\Gamma(\Sigma^+ \to p\gamma)$ to possible changes in b_2/b_1. This is given in Figs. 3 and 4 for $\Sigma^+ \to pe^+e^-$ and $\Sigma^+ \to p\mu^+\mu^-$ respectively, for $c_1 = c_2 = 0$. The $\Sigma^+ \to p\mu^+\mu^-$ is the more sensitive probe. We have checked the sensitivity of these ratios to b_2/b_1 for other values of c_1, c_2 as well. Only for values of $|c_1/b_1|$ of the order of 5-10 and very large $|c_2/b_1|$ values of the order of 10^2, can one perceive sizeable deviations from the results given for $c_2 = c_1 = 0$. However, as it will be shown in the course of this analysis, such large values for c_1/b_1 and c_2/b_1 are unlikely. We have also checked the implications of positive values of b_2/b_1 (again very unlikely in the light of the presently known value for it) and we found, as expected, that the partial decay rates for $\Sigma^+ \to pe^+e^-$ are not seriously affected. Using, for example, $c_1 = 0$, $c_2/b_1 = 10$, $\Gamma(\Sigma^+ \to pe^+e^-)/\Gamma(\Sigma^+ \to p\gamma)$ changes from 7.34×10^{-3} for $b_2/b_1 = 1$ to 7.98×10^{-3} for $b_2/b_1 = -0.5$ and to 8.25×10^{-3} for $b_2/b_1 = -1$. On the other hand, $\Gamma(\Sigma^+ \to p\mu^+\mu^-)/\Gamma(\Sigma^+ \to p\gamma)$ changes from 1.13×10^{-5} for $b_2/b_1 = 1$ to 6.15×10^{-5} for $b_2/b_1 = -0.5$ and 8.05×10^{-5} for $b_2/b_1 = -1$. In any case with a better determination of $\alpha(\Sigma^+ \to p\gamma)$, the uncertainty in the b_2/b_1 value will diminish and it will be possible to use the partial decay rates to the leptonic modes as a cleaner probe for the magnitude of c_1, c_2 free from the uncertainty due to a loose b_2/b_1 value.

For a given value of b_2/b_1, as measured in $\Sigma^+ \to p\gamma$ decay, the expressions (23), (24) are quadratic functions of $x = c_1/b_1$, $y = c_2/b_1$. There are minima of these functions for certain values $x^{e,\mu}_{min}$, $y^{e,\mu}_{min}$ which, if disproved experimentally, would show that one or more of our initial assumptions is to be amended [e.g., the reality of b_1, b_2, some strong form factor dependence or the possible manifestation of an exotic particle in the $\ell^+\ell^-$ channel[35)]. In fact, we know that the form factors involved have imaginary parts due to real processes like $\Sigma^+ \to n\pi^+ \to p\ell^+\ell^-$. The imaginary parts of b_1, b_2 have been estimated by Kogan and Shifman[13)] and found to be very small for $\Sigma^+ \to p\gamma$. Hence, we expect that the limits we derive from (23) and (24) are quite reliable indeed. Using $b_2/b_1 = -0.42$, the absolute lower limits for the $\Sigma^+ \to pe^+e^-$, $\Sigma^+ \to p\mu^+\mu^-$ decays are then

$$\frac{\Gamma(\Sigma^+ \to pe^+e^-)}{\Gamma(\Sigma^+ \to p\gamma)} \geq \frac{1}{138} = 7.2\times10^{-3} \tag{25}$$

with the equality holding for $x^e_{min} = 0.70$, $y^e_{min} = -11.9$ and

$$\frac{\Gamma(\Sigma^+ \to p\mu^+\mu^-)}{\Gamma(\Sigma^+ \to p\gamma)} \geq \frac{1}{1.67\times10^5} = 6.0\times10^{-6} \tag{26}$$

with lowest value holding for $x^{\mu}_{min} = 0.68$, $y^{\mu}_{min} = -8.0$.

The minimal value for $\Sigma^+ \to pe^+e^-$ is within 3% of the value which obtains with $x = y = 0$, while for $\Sigma^+ \to p\mu^+\mu^-$ the minimal value of $\Gamma(\Sigma^+ \to p\mu^+\mu^-)/\Gamma(\Sigma^+ \to p\gamma)$ is nearly three times smaller than the value of 1.63×10^{-5} which is obtained with $x = y = 0$. To underline the large difference in the sensitivity of these two decays to the values of x and y, we give in Fig. 5 $\Gamma(\Sigma^+ \to pe^+e^-)/\Gamma(\Sigma^+ \to p\gamma)$ as a function of $y = c_2/b_1$ for $x = x^{e}_{min}$ and in Fig. 6 we display $\Gamma(\Sigma^+ \to p\mu^+\mu^-)/\Gamma(\Sigma^+ \to p\gamma)$ as a function of $y = c_2/b_1$ for $x = x^{\mu}_{min}$. With this we exhausted the information obtainable from the decay rate and we turn now to the various distributions.

We start with the $s = q^2$ distribution of the $\Sigma^+ \to p\mu^+\mu^-$ decay. All the curves of a certain plot, for all distributions of this type given below, are normalized to the same value for ease of comparison. In Fig. 7 we plot $d(\Sigma^+ \to p\mu^+\mu^-)/ds$ for several values of the couple of form factor ratios x, y ($x = c_1/b_1$, $y = c_2/b_1$) and for the canonical value $b_1/b_2 = -0.42$. Unless otherwise specified, this value of b_1/b_2 is used in all curves. Generally, when x, y are nearly equal, the distributions look very much alike even for fairly large values of $x \approx y$. On the other hand, when $|y| >> |x|$, the distributions are pulled towards high s values. The curves we give here are typical from among a variety we checked[34]. Only if b_2/b_1 changes significantly from the presently accepted value, there is more discernible variations in the curves for $x \approx y$, as shown in Fig. 8. The same type of information may be extracted if the curves are expressed in terms of the proton recoil momentum [see Eqs. (17) and (18)] and this is shown in Fig. 9. A similar analysis was performed for $\Sigma^+ \to pe^+e^-$ and an example is given in Fig. 10. The pattern is similar to the one described for $\Sigma^+ \to p\mu^+\mu^-$, though differences are less pronounced, unless c_1, c_2 are very large ($\simeq 50\ b_1$).

We turn now to the asymmetry distributions presented in (19) to (22). To give an idea on the sensitivity of the angular distribution to the size of the coupling constants ratios, we present several plots of V(s,t) and W(s,t) for various values of c_1/b_1, c_2/b_1,. An extensive display of the variation of V(s,t), W(s,t) for various ranges of s and t and for different assumptions for c_1/b_1, c_2/b_1 can be found in Ref. 34). A representative sample of this is given in Figs. 11-14.

In Fig. 11 we plot V(s,t) the proton angular asymmetry function for several combinations of c_1/b_1, c_2/b_1 and constant $s = 4.8\times10^4$ MeV^2 as a function of t; in Fig. 12 we give a similar plot for W(s,t) the positron angular asymmetry function at $s = 6.25\times10^4$ MeV^2. Both these figures are for the decay $\Sigma^+ \to pe^+e^-$. We checked[34] that the depicted trend does not change appreciably when one varies s over its range. As the curves show, the W-asymmetry of the positron is sensibly larger than the V-asymmetry of the proton in the $\Sigma^+ \to pe^+e^-$ decay; unfortunately it shows no sensitivity to changes in c_i/b_1, contrary to the behaviour of V(s,t).

Turning to the $\Sigma^+ \to p\mu^+\mu^-$ decay, we give in Fig. 13 the V(s,t) function for $s = 6.25\times10^4$ MeV^2 and three different combinations of c_1/b_1 and c_2/b_1. One should remark again the strong variation as a function of t for the case that the c_i's are different from zero and as large or larger than b_1. In Fig. 14 we show W(s,t) for the $\Sigma^+ \to p\mu^+\mu^-$ decay as a function of t, for several values of s, with $c_1 = c_2 = 0$. The variation on s is fairly typical for other choices of the pair of coupling constants as well[34].

From the experimental point of view, it is more advantageous to integrate over t, since one does not expect large numbers of events in the near future. We find again that the more sensitive decay is $\Sigma^+ \to p\mu^+\mu^-$. In Fig. 15 we depict for $\Sigma^+ \to p\mu^+\mu^-$ and for several choices of values for c_1/b_1, c_2/b_1 the directly measurable quantity $\bar{\alpha}(s)$ which we define [see Eq. (19)] as

$$\bar{\alpha}(s) = \frac{\int_{t_{min}}^{t_{max}} F(s,t)\, V(s,t)\, dt}{\int_{t_{min}}^{t_{max}} F(s,t)\, dt} \qquad (27)$$

For large c_1/b_1, c_2/b_1 a sizeable asymmetry is observed.

4. - DISCUSSION

The mechanisms operating in the various transitions namely the identification of the correct operators in the Wilson expansion and their evaluation between hadronic states including corrections by the strong interactions, as well as the estimate of long distance effects, are the big issues to be still resolved in the realm of electroweak non-leptonic interactions. With the aim of

contributing to the elucidation of these issues, we studied the phenomenology of $\Sigma \to p\ell^+\ell^-$ transitions; it appears that detailed measurements on both $\Sigma^+ \to pe^+e^-$ and $\Sigma^+ \to p\mu^+\mu^-$ have indeed the potential we envisage.

The hadronic electroweak transitions involve magnetic type and charge radius type parts. So far, these two types of transitions were investigated separately: the magnetic transition was observed experimentally and studied extensively theoretically in the baryonic decays $B \to B'\gamma$[7)-20)], while the mesonic $K^+ \to \pi^+\ell^+\ell^-$ mode[36)] is the standard for the study of the charge radius electroweak transition[37),38)]. It should be reminded, however, that the interpretation of the latter in terms of basic mechanisms is beset with difficulties[37),38)].

The $\Sigma^+ \to p\ell^+\ell^-$ decay presents the opportunity of studying both types of transitions in the same decay, thus imposing a considerably more constrained framework for the confrontation of theoretical models. In fact, $\Sigma^+ \to p\ell^+\ell^-$ is kind of unique in affording this type of exercise, being the only one from among the observed $B' \to B\gamma$ decays (B', B of spin-$\frac{1}{2}$) which has enough phase space to allow for both e^+e^- and $\mu^+\mu^-$ decays. As our analysis reveals, the detection and comparison of both decays would be most advantageous. The only other decay having enough phase space, $\Sigma^0 \to n\gamma$, is much more difficult to measure. The decay $\Omega^-(3/2^+) \to \Xi^-(\frac{1}{2}^+)\ell^+\ell^-$ has also sufficient phase space for this type of analysis but entails a more involved amplitude structure and will be discussed separately[39)].

There are no calculations so far, to the best of our knowledge, of both the magnetic and charge radius form factors of relevance for $B' \to B\gamma$ decays, on either the quark or the hadronic level. An exception is the estimate of the free quark model contribution[26)] to $\Sigma^+ \to p\ell^+\ell^-$. However, one knows that at least in the $\Sigma^+ \to p\gamma$, the contribution of the single quark transition is of minor relevance[10),13),15),16)]. We shall return to this point and show that the same holds for the charge radius transition, in contradiction to the conclusion of Chia and Rajagopal[26)].

Firstly, the experimental situation. There is only one experiment[40)], using a hydrogen bubble chamber in which $\Sigma^+ \to pe^+e^-$ was detected. Three events were observed with invariant mass of the e^+e^- pair between ~1.5 and ~2.5 MeV[35),40)]. They were considered consistent with photo-conversion from $\Sigma^+ \to p\gamma$ and the rate is given as

$$\left.\frac{\Gamma(\Sigma^+ \to p e^+ e^-)}{\Gamma(\Sigma^+ \to p\gamma)}\right|_{exp} \simeq \frac{1}{140} \,. \tag{28a}$$

This figure is consistent with our result in Table 1 for the internal conversion (IC) part which obtains for $c_1 = c_2 = 0$,

$$\frac{\text{I.C.}\,\Gamma(\Sigma^+ \to p e^+ e^-)_{th}}{\Gamma(\Sigma^+ \to p\gamma)} = \frac{1}{134} \,. \tag{28b}$$

The occurrence of the events in the region $s < 6\ \text{MeV}^2$ is consistent with the expectation from curve A in Fig. 10, but also, of course, indistinguishable from curve B.

Identifying the three events as due to internal conversion, the authors of Ref. 40) give also an upper limit for the "neutral current" decay (NC), i.e., the events due to the form factors of Eq. (5)

$$\frac{\text{N.C.}\,\Gamma(\Sigma^+ \to p e^+ e^-)}{\Gamma(\Sigma^+ \to p\gamma)} < \frac{1}{175} = 5.7 \times 10^{-3} \,. \tag{29}$$

For the decay $\Sigma^+ \to p\mu^+\mu^-$ no useful limits are available.

Our Table 1 shows the sensitivity of the absolute rate of $\Sigma^+ \to pe^+e^-$ to the size of c_1/b_1, c_2/b_1, given the established ratio $(b_1/b_2) = -0.42$ [cf. Eq. (8)]. The value in (28a) is practically at the absolute minimum determined in (25) which holds for $c_1/b_1 = 0.7$, $c_2/b_1 = -11.9$. However, the existing value (28a) is not a high accuracy result. If an improved experiment will find a ratio substantially lower than (25), this would signal new physics.

The above remarks are quite stable against possible experimental changes in the value of the asymmetry parameter α, since the $\Sigma^+ \to pe^+e^-$ rate is only slightly affected by changes in b_2/b_1. For instance, a variation of the b_2/b_1 value (8) between -0.7 and -0.2 affects $\Gamma(\Sigma^+ \to pe^+e^-)/\Gamma(\Sigma^+ \to p\gamma)$ by at most a few percent (see Fig. 3), as long as $|c_1/b_1| \lesssim 10$, $|c_2/b_1| \lesssim 50$.

We turn now to using (28a) to obtain limits on the values of c_1, c_2. From (23) and allowing for the uncertainty in (28a) by using $\Gamma(\Sigma^+ \to pe^+e^-)/\Gamma(\Sigma^+ \to p\gamma)|_{exp} \lesssim 1/120$, we determine

$$\left|\frac{c_1}{b_1}\right| \lesssim 5 \; ; \quad \left|\frac{c_2}{b_1}\right| \lesssim 10 \; . \tag{30}$$

A precise determination of the $\Sigma^+ \to pe^+e^-$ rate would lead to a more restricted two-dimensional area for the possible values of c_1/b_1, c_2/b_1.

Using now (24), we exploit the limits (30) to restrict the expected $\Sigma^+ \to p\mu^+\mu^-$ rate to obey (see Table 2)

$$\frac{\Gamma(\Sigma^+ \to p\mu^+\mu^-)}{\Gamma(\Sigma^+ \to pe^+e^-)} \lesssim \frac{1}{120} \; . \tag{31a}$$

Here again, a violation of this upper limit would signal new physics. It may arise from the existence of an exotic particle like the axion[35] or some unexpected large variation of the form factors which were assumed to be essentially constant in the range of interest here, according to standard knowledge. An actual measurement of the muonic mode will determine much better the c_1, c_2 couplings in view of the sensitivity of this mode to changes in their values. So far, a combination of (26), (28a) and (31a) allows us to constrain the rate of the $\Sigma^+ \to p\mu^+\mu^-$ mode within broad limits

$$\frac{1}{1210} \lesssim \frac{\Gamma(\Sigma^+ \to p\mu^+\mu^-)}{\Gamma(\Sigma^+ \to pe^+e^-)} \lesssim \frac{1}{120} \; . \tag{31b}$$

As we already mentioned, there are no calculations of the c_i form factors in the literature. On the other hand, from the analysis of $\Sigma^+ \to p\gamma$[8)-13)] one has learned that at the quark level, the calculation of the b_1, b_2 couplings should take into account the contributions of all diagrams of Fig. 1. The simplest is the single quark transition $s \to d\gamma$ which we define with the aid of the induced vertex Γ_μ

$$\Gamma_\mu = -\frac{e}{(4\pi)^2} \cdot \frac{g^2}{2M_W^2} \bar{d}\left[F_1\left(q_\mu \not{q} - q^2\gamma_\mu\right)\frac{1-\gamma_5}{2}\right.$$

$$\left. + i F_2 \sigma_{\mu\nu} q^\nu \left(m_s \frac{1+\gamma_5}{2} + m_d \frac{1-\gamma_5}{2}\right)\right] s \; . \tag{32}$$

In the free quark model (FQ)[24)-26)], one has ${}^{(FQ)}F_2/{}^{(FQ)}F_1 \simeq -3\times10^{-4}$, the magnetic part being thus negligible compared to the charged radius one (which does not appear, however, in real photon transitions). When QCD corrections are added, F_2 is dramatically increased[5),6)], as the free quark suppression factors

like $(m_c^2-m_u^2)/M_W^2$ are replaced for the two-loop graphs by factors like $\ln(m_c^2/\mu^2)$, μ being a renormalization scale. The QCD corrected form factors of the quark model (QC) are obtained in the leading log approximation to leading order in α_s and for quark masses smaller than M_W [see Ref. 41) for $^{(QC)}F_1$ and Ref. 6) for $^{(QC)}F_2$]:

$$^{(QC)}F_1 \simeq -\frac{8K}{9}\left[V_{sc}V_{dc}\ln\frac{m_c}{\mu}+V_{st}V_{dt}\ln\frac{m_t}{m_c}\right] \quad (33a)$$

$$= -0.38\,K,$$

$$^{(QC)}F_2 \simeq \frac{8\alpha_s}{3\pi}\left[V_{ud}V_{us}\ln\frac{m_c}{\mu}+V_{st}V_{dt}\ln\frac{m_t}{m_c}\right] \quad (33b)$$

$$= 0.36\,.$$

$V_{k\ell}$ are the Kobayashi-Maskawa matrices. The QCD correction to F_1 which we denoted by K was calculated by several authors[27),41)] to be between (-0.5) and (-2.5). We shall use here K = -1. In the numerical estimates for $^{(QC)}F_1$ and $^{(QC)}F_2$ we used μ = 250 MeV (the inverse confinement radius), m_c = 1.7 GeV, m_t = 50 GeV and $V_{k\ell}$'s were taken from Ref. 42).

In order to calculate the contribution of the QCD corrected single quark transition to $\Sigma^+ \to p\ell^+\ell^-$, we adopt the model of Ref. 10) whereby the hadrons are described by SU(6) quark model wave functions and we use overlap factors (to the quark operators of $s \to d\gamma$) of 1. Then we obtain relations between the hadronic form factors b_i, c_i of the $\Sigma^+ \to p"\gamma"$ vertex (3) and the form factors of the $s \to d\gamma$ vertex (32), taking $(m_d/m_s) \to 0$,

$$b_1 = \frac{m_s F_2 m_p^{1/2}}{24\pi^2 m_\Sigma^{1/2}}; \quad c_1 = \frac{(m_\Sigma - m_p) F_1 m_p^{1/2}}{6\pi^2 m_\Sigma^{1/2}} \quad (34)$$

and similar expressions for b_2, c_2. Using now the values of (33), one finds $^{(QC)}c_1/^{(QC)}b_1 = 6.1$ for m_s = 175 MeV[43)] and $^{(QC)}c_1 = -^{(QC)}c_2$. However, it is known that $^{(QC)}F_2$ cannot[13),16)] account for the observed $\Sigma^+ \to p\gamma$ transition by quite a large factor, in fact from (8), (33b) and (34) one finds

$$\left|\frac{^{(exp)}b_1}{^{(QC)}b_1}\right| = 29. \quad (35)$$

This conclusion is supported by the value of the asymmetry parameter (7c) which would be $\simeq$ 1 for a dominant single quark transition. The charge radius form factors in the QCD corrected single quark model are then from (33)-(35)

$$(QC)c_1 = -(QC)c_2 = 0.21\,(exp)b_1 \qquad (36)$$

and their contribution to the $\Sigma^+ \to p\ell^+\ell^-$ rates is rather negligible. Using (15) with $b_2 = b_1 = 0$, one finds with the values of c_i from (36) that $^{(NC)}\Gamma(\Sigma^+ \to pe^+e^-) = 1.6\times10^{-14}$ eV, nearly four orders of magnitude below the experimental limit (29). Even if $K \simeq (-2) \neq (-3)$, the overall picture is not changed and we conclude that the single quark transition is of minor effect also in the $\Sigma^+ \to p\ell^+\ell^-$ decays*).

The long distance contributions have been considered in Ref. 13) in connection with $\Sigma^+ \to p\gamma$. These authors have estimated the contributions of the imaginary part coming from real intermediate states and of the logarithmic terms in the real part of the amplitude and found them to be negligibly small. Hence, it is safe to predict that also in the charge radius part of the $\Sigma^+ \to p''\gamma''$ transition, the two-quark contribution (Fig. 1b) will play the major role. This opens the possibility of a tighter check for a complete calculation of both parts of the $\Sigma^+ \to p\ell^+\ell^-$ transitions, including $\Sigma^+ \to p\gamma$. Such calculation is still lacking. Nonetheless, some information on the c_i form factors and their underlying mechanism has already been derived here. More will be obtained only when detailed measurements become available, particularly of the rarer $\Sigma^+ \to p\mu^+\mu^-$ mode.

ACKNOWLEDGEMENTS

P.S. acknowledges the hospitality of the SLAC Theory Group during the summer of 1986 when part of this work was performed and the hospitality and support of Theory Division at CERN. This research was supported at the Technion by the Fund for Promotion of Research.

---

*) On this point we disagree with the result[26] that this contribution can be as high as $\sim10^{-11}$ eV. The large rate deduced from Eq. (18) of Ref. 26) is due to the omission of a factor α and to the error of the approximate expression for the three-body phase space, amplified by the use of a strange quark mass of 510 MeV.

Table 1

The ratio $\Gamma(\Sigma^+ \to p\gamma)/\Gamma(\Sigma^+ \to pe^+e^-)$ for different values of c_1/b_1, c_2/b_1 and $b_1/b_2 = -0.42$.

-50	-10	-1	-0.5	0	0.5	1	10	50	c_1/b_1 / c_2/b_1
11	62	79.6	80.0	80.0	80.3	80.2	65	11	50
11	86	125.2	125.9	126	126.7	126.6	93	11	10
11	88.8	132.2	133.1	133.4	133.9	133.9	96.8	11	1
11	89	132.5	133.4	133.7	134.2	134.2	97	11	0.5
11	89	132.8	133.7	134	134.5	134.5	97	11	0
11	89.2	133.1	134	134.3	134.8	134.8	97.3	11	-0.5
11	89.3	133.4	134.2	134.6	135.1	135.1	97.4	11	-1
11	91	136.2	137.1	138.0	138.0	137.9	99	11	-10
11	77	107.3	108	109	108.4	108.4	83	11	-50

Table 2

The ratio $\Gamma(\Sigma^+ \to pe^+e^-)/\Gamma(\Sigma^+ \to p\mu^+\mu^-)$ for different values of c_1/b_1, c_2/b_1 and $b_1/b_2 = -0.42$.

-10	-5	-1	-0.5	0	0.5	1	5	10	c_1/b_1 / c_2/b_1
88	116	137	138	140	140	139	123	95	10
106	162	221	230	234	235	235	185	118	5
120	215	369	384	396	400	400	261	136	1
121	220	394	412	426	431	429	272	138	0.5
124	227	422	442	458	464	462	285	141	0
124	235	452	475	494	501	499	395	143	-0.5
127	233	484	512	533	541	540	308	145	-1
134	293	812	898	948	1001	980	402	158	-5
136	299	869	972	1050	1095	1097	416	156	-10

REFERENCES

1) Y. Hara, Phys. Rev. Lett. 12 (1964) 378;
S.Y. Lo, Nuov. Cimento 37 (1965) 753.

2) M.K. Gaillard and P. Roy, Phys. Lett. 38B (1972) 245.

3) R.H. Graham and S. Pakvasa, Phys. Rev. 140B (1965) 1144;
M.K. Gaillard, Nuov. Cim. 6A (1971) 559;
B.R. Holstein, Nuov. Cim. 2A (1971) 561;
G. Farrar, Phys. Rev. D4 (1971) 212.

4) M.A. Ahmed and G.G. Ross, Phys. Lett. 59B (1976) 293.

5) N. Vasanti, Phys. Rev. D13 (1976) 1889.

6) M.A. Shifman, A.I. Vainshtein and V.I. Zacharov, Phys. Rev. D18 (1978) 2583.

7) M.D. Scadron and L.R. Thebaud, Phys. Rev. D8 (1973) 2190;
M.D. Scadron and M. Visinescu, Phys. Rev. D28 (1983) 1117;
W.F. Kao and H.J. Schnitzer, Phys. Lett. 183B (1987) 361.

8) F.E. Close and H.R. Rubinstein, Nucl. Phys. B173 (1980) 477;
M.B. Gavela et al., Phys. Lett. 101B (1981) 417;
G. Nardulli, Phys. Lett. 190B (1987) 187.

9) I. Picek, Phys. Rev. D21 (1980) 3169;
K.G. Rauh, Z. Phys. C - Particles and Fields 10 (1981) 81;
Yu.I. Skovpen', Sov. J. Nucl. Phys. 34 (1981) 773.

10) F. Gilman and M.B. Wise, Phys. Rev. D19 (1979) 976.

11) A.N. Kamal and R.C. Verma, Phys. Rev. D26 (1982) 190;
A.N. Kamal and Riazuddin, Phys. Rev. D28 (1983) 2317.

12) C.-H. Lo, Phys. Rev. D26 (1982) 199.

13) Ya. I. Kogan and M.A. Shifman, Sov. J. Nucl. Phys. 38 (1983) 628.

14) J.O. Eeg, Z. Phys. C - Particles and Fields 21 (1984) 253;
S.G. Kamath, Nucl. Phys. B198 (1982) 61.

15) M.K. Gaillard, X.Q. Li and S. Rudaz, Phys. Lett. 158B (1985) 158.

16) L. Bergström and P. Singer, Phys. Lett. 169B (1986) 297.

17) L.K. Gerschwin et al., Phys. Rev. 188 (1969) 2077;
A. Manz et al., Phys. Lett. 96B (1980) 217.

18) S.F. Biagi et al., Z. Phys. C - Particles and Fields 30 (1986) 201.

19a) C. James et al., contribution from FERMILAB to the XXIII International Conf. on High Energy Physics, Berkeley, July 1986.

19b) S.F. Biagi et al., Lausanne preprint (December 1986).

20) M. Bourquin et al., Nucl. Phys. B241 (1984) 1.

21) M.A. Shifman, A.I. Vainshtein and V.I. Zacharov, Nucl. Phys. B120 (1977) 316;
F.J. Gilman and M.B. Wise, Phys. Rev. D20 (1979) 2392.

22) P. Singer, Proc. Intern. Symposium on Production and Decay of Heavy Flavours, Heidelberg, May 1986, Eds. K.R. Shubert and R. Waldi, p, 293 (1986).

23) B.W. Lee and M.K. Gaillard, Phys. Rev. D10 (1974) 897.

24) E. Ma and A. Pramudita, Phys. Rev. D24 (1981) 1410;
N. Deshpande and G. Eilam, Phys. Rev. D26 (1982) 2463.

25) T. Inami and C.S. Lim, Prog. Theor. Phys. 65 (1981) 297.

26) S.-P. Chia and G. Rajagopal, Phys. Lett. 156B (1985) 405.

27) E. Witten, Nucl. Phys. B120 (1977) 387;
J.O. Eeg, Phys. Rev. D23 (1981) 2596.

28) We follow the conventions of J.D. Bjorken and S.D. Drell, Relativistic Quantum Fields (Mc Graw Hill, New York, 1967).

29) S.D. Drell and F. Zachariasen, Electromagnetic Structure of Nucleons (Oxford Univ. Press, London, 1961), Ch. I.

30) I.V. Lyagin and E.Kh. Ginzburg, Soviet Physics JETP 14 (1962) 653.

31) Particle Data Group, Phys. Lett. 170B (1986) 1.

32) K. Miyake et al., Proceedings of the International Symp. on Lepton and Photon Interactions at High Energies, Kyoto, August 1985, Eds. M. Konuma and K. Takahashi, p. 930 (1985).

33) J.C. D'Olivo and M.A. Pérez, Phys. Rev. D23 (1981) 1994.

34) R. Safadi, "Weak Radiative Decays of Baryons", M.Sc. Thesis, Technion, (1986).

35) M. Suzuki, Phys. Lett. 175B (1986) 364.

36) P. Bloch et al., Phys. Lett. 56B (1975) 201.

37) L. Bergström and P. Singer, Phys. Rev. Lett. 55 (1985) 2633.

38) G. Ecker, A. Pich and E. de Rafael, Nucl. Phys. B (to be published);
see here for references to previous theoretical analyses.

39) R. Safadi and P. Singer, to be published.

40) C. Ang et al., Z. Phys. 228 (1969) 151.

41) F.J. Gilman and M.B. Wise, Phys. Rev. D21 (1980) 3150.

42) K. Kleinknecht and B. Renk, Z. Phys. C - Particles and Fields 34 (1987) 209.

43) J. Gasser and H. Leutwyler, Physics Reports 87C (1982) 77.

FIGURE CAPTIONS

Fig. 1 : Typical quark diagrams in the short distance description of non-leptonic radiative decays; the black box stands for the effective electroweak interaction as modified by QCD corrections.
(a) The one quark $s \to d\gamma$ transition;
(b)(c) Two-quark and three-quark transitions.
(The photon may be virtual.)

Fig. 2 : The effective diagram for the decay $\Sigma^+ \to p\ell^+\ell^-$.

Fig. 3 : The ratio $\Gamma(\Sigma^+ \to pe^+e^-)/\Gamma(\Sigma^+ \to p\gamma)$ versus b_2/b_1 for $c_1 = c_2 = 0$.

Fig. 4 : The ratio $\Gamma(\Sigma^+ \to p\mu^+\mu^-)/\Gamma(\Sigma^+ \to p\gamma)$ versus b_2/b_1 for $c_1 = c_2 = 0$.

Fig. 5 : The ratio $\Gamma(\Sigma^+ \to pe^+e^-)/\Gamma(\Sigma^+ \to p\gamma)$ as a function of $y = c_2/b_1$ at $x^e_{min} = 0.7$ and $b_2/b_1 = -0.42$.

Fig. 6 : The ratio $\Gamma(\Sigma^+ \to p\mu^+\mu^-)/\Gamma(\Sigma^+ \to p\gamma)$ as a function of $y = c_2/b_1$ at $x^\mu_{min} = 0.68$ and $b_2/b_1 = -0.42$.

Fig. 7 : The invariant mass distribution of the lepton pair in the decay $\Sigma^+ \to p\mu^+\mu^-$ for different values of c_1/b_1, c_2/b_2 ($b_1/b_2 = -0.42$). The parameters of the curves are: $c_1 = c_2 = 0$ (A); $c_1/b_1 = c_2/b_1 = 5$ (B); $c_1/b_1 = c_2/b_1 = -5$ (C); $c_1 = 0$, $c_2/b_1 = 50$ (D).

Fig. 8 : The invariant mass distribution of the lepton pair in the decay $\Sigma^+ \to p\mu^+\mu^-$ for different values of c_1/b_1, c_2/b_1 and $\alpha(\Sigma^+ \to p\gamma)$. The parameters of the curves are: $c_1 = c_2 = 0$, $\alpha(\Sigma^+ \to p\gamma) = -0.72$ (A); $c_1 = c_2 = 0$, $\alpha(\Sigma^+ \to p\gamma) = -0.1$ (A1); $c_1 = 0$, $c_2/b_1 = 50$, $\alpha(\Sigma^+ \to p\gamma) = -0.72$ (B); $c_1 = 0$, $c_2/b_1 = 50$, $\alpha(\Sigma^+ \to p\gamma) = -0.1$ (B1).

Fig. 9 : The distribution of the recoil proton momentum in the decay $\Sigma^+ \to p\mu^+\mu^-$ for different values of c_1/b_1, c_2/b_1. The parameters of the curves are: $c_1 = c_2 = 0$ (A); $c_1/b_1 = c_2/b_1 = -5$ (B); $c_1 = 0$, $c_2/b_1 = 50$ (C).

Fig. 10: The invariant mass distribution of the lepton pair in the decay $\Sigma^+ \to pe^+e^-$ for different values of c_1/b_1, c_2/b_1. The parameters of the curves are: $c_1 = c_2 = 0$ (A); $c_1/b_1 = c_2/b_1 = -5$ (B); $c_1/b_1 = 50$, $c_2 = 0$ (C); $c_1/b_1 = c_2/b_1 = 50$ (D).

Fig. 11: The proton angular asymmetry function V(s,t) [Eqs. (19) and (21)] versus t in the decay $\Sigma^+ \to pe^+e^-$ for constant s. The parameters of the curves are: $c_1 = c_2 = 0$ (A); $c_1/b_1 = 5$, $c_2 = 0$ (B); $c_1/b_1 = -5$, $c_2 = 0$ (C).

Fig. 12: The e^+ angular asymmetry function W(s,t) [Eqs. (19) and (22)] versus t in the decay $\Sigma^+ \to pe^+e^-$ for constant s. The parameters of the curves are: $c_1 = c_2 = 0$ (A); $c_1/b_1 = c_2/b_1 = -5$ (B): $c_1 = 0$, $c_2/b_1 = -5$ (C).

Fig. 13: The proton angular asymmetry function V(s,t) [Eqs. (19) and (21)] versus t in the decay $\Sigma^+ \to p\mu^+\mu^-$ for constant $s = 6.25\times10^4$ MeV^2. The parameters of the curves are: $c_1 = c_2 = 0$ (A); $c_1/b_1 = c_2/b_1 = -5$ (B); $c_1/b_1 = -5$, $c_2 = 0$ (C).

Fig. 14: The μ^+ angular asymmetry function W(s,t) [Eqs. (19) and (22)] versus t in the decay $\Sigma^+ \to p\mu^+\mu^-$ for $c_1 = c_2 = 0$ and different values of constant s: $s = 4.6\times10^4$ MeV^2 (A); $s = 4.8\times10^4$ MeV^2 (B); $s = 5.1\times10^4$ MeV^2 (C); $s = 6\times10^4$ MeV^2 (D).

Fig. 15: The t-integrated asymmetry function $\bar{\alpha}(s)$ [Eq. (27)] in the decay $\Sigma^+ \to p\mu^+\mu^-$. The parameters of the curves are: $c_1 = c_2 = 0$ (A); $c_1/b_1 = -c_2/b_1 = 5$ (B); $c_1/b_1 = -c_2/b_1 = 10$ (C).

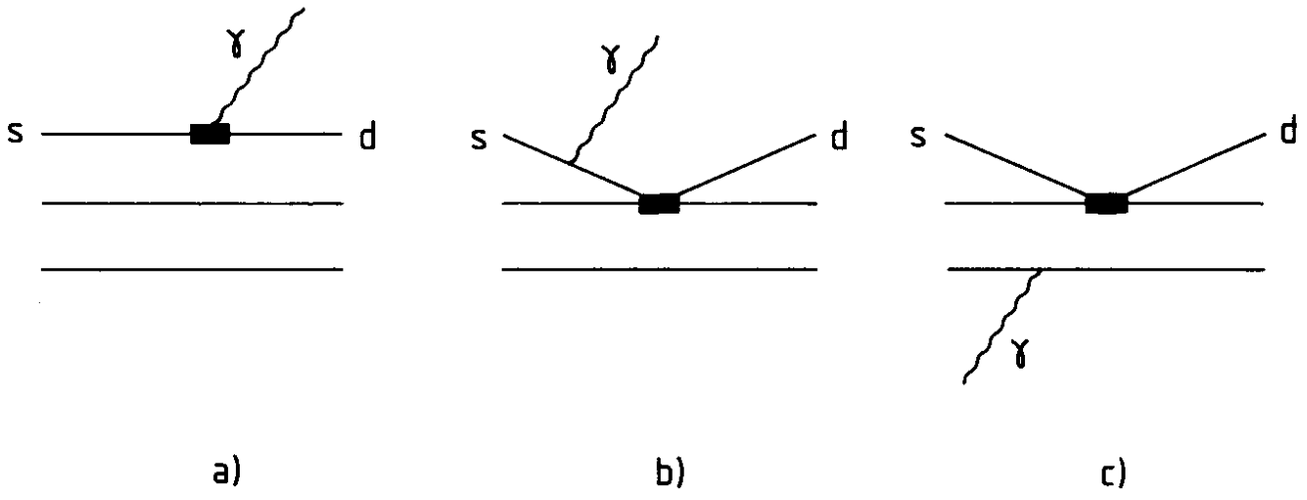

Fig. 1

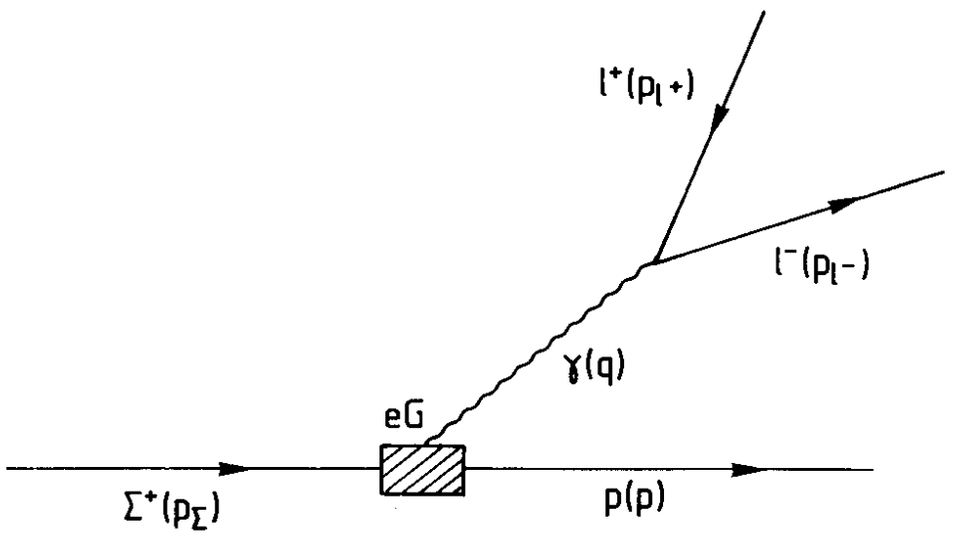

Fig. 2

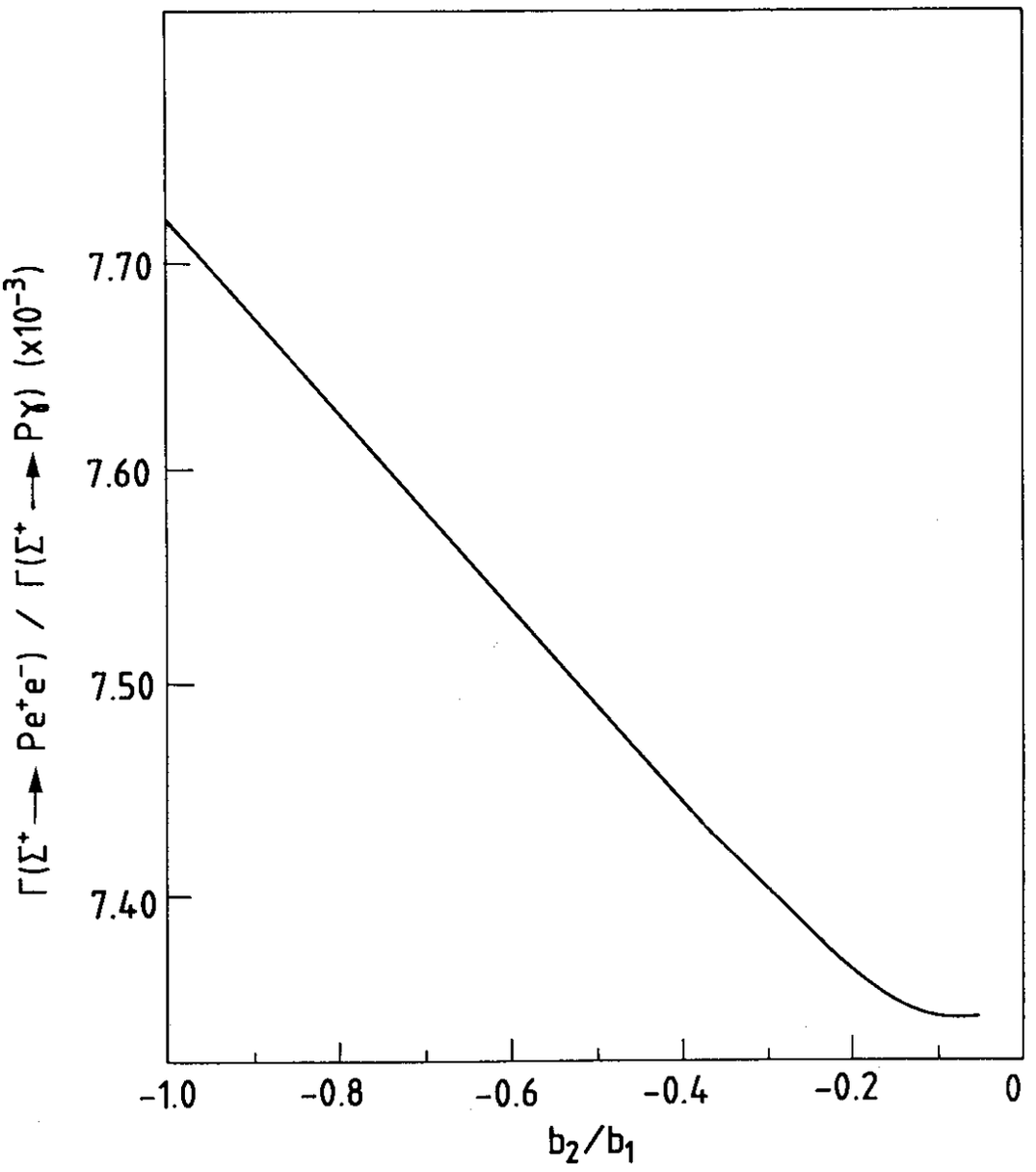
$\Gamma(\Sigma^+ \rightarrow Pe^+e^-) / \Gamma(\Sigma^+ \rightarrow P\gamma)$ $(x10^{-3})$
7.70
7.60
7.50
7.40
-1.0
-0.8
-0.6
-0.4
-0.2
0
b_2/b_1

Fig. 3

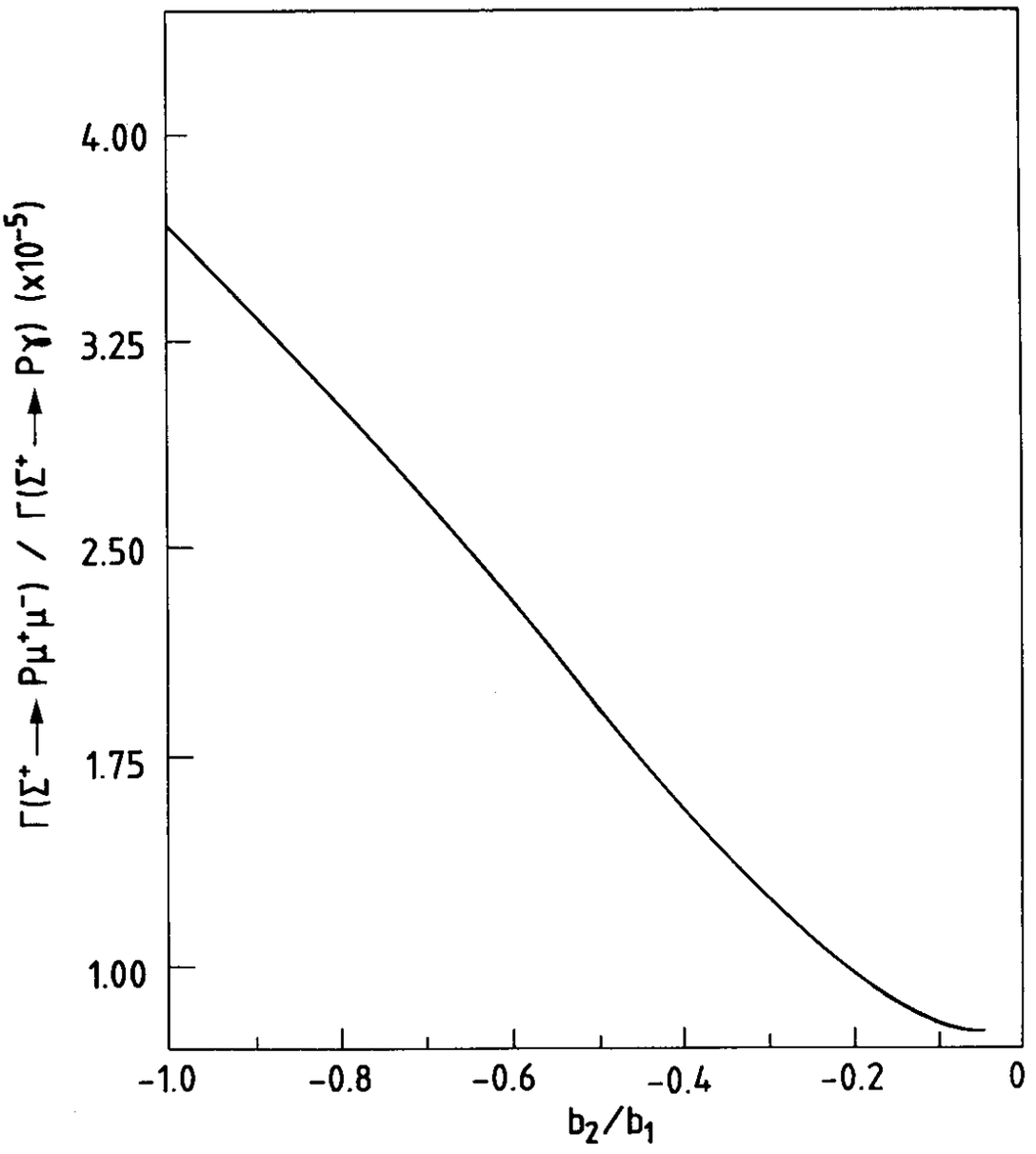
4.00
3.25
2.50
1.75
1.00
-1.0
-0.8
-0.6
-0.4
-0.2
0
b_2/b_1
$\Gamma(\Sigma^+ \to P\mu^+\mu^-) / \Gamma(\Sigma^+ \to P\gamma)$ $(x10^{-5})$

Fig. 4

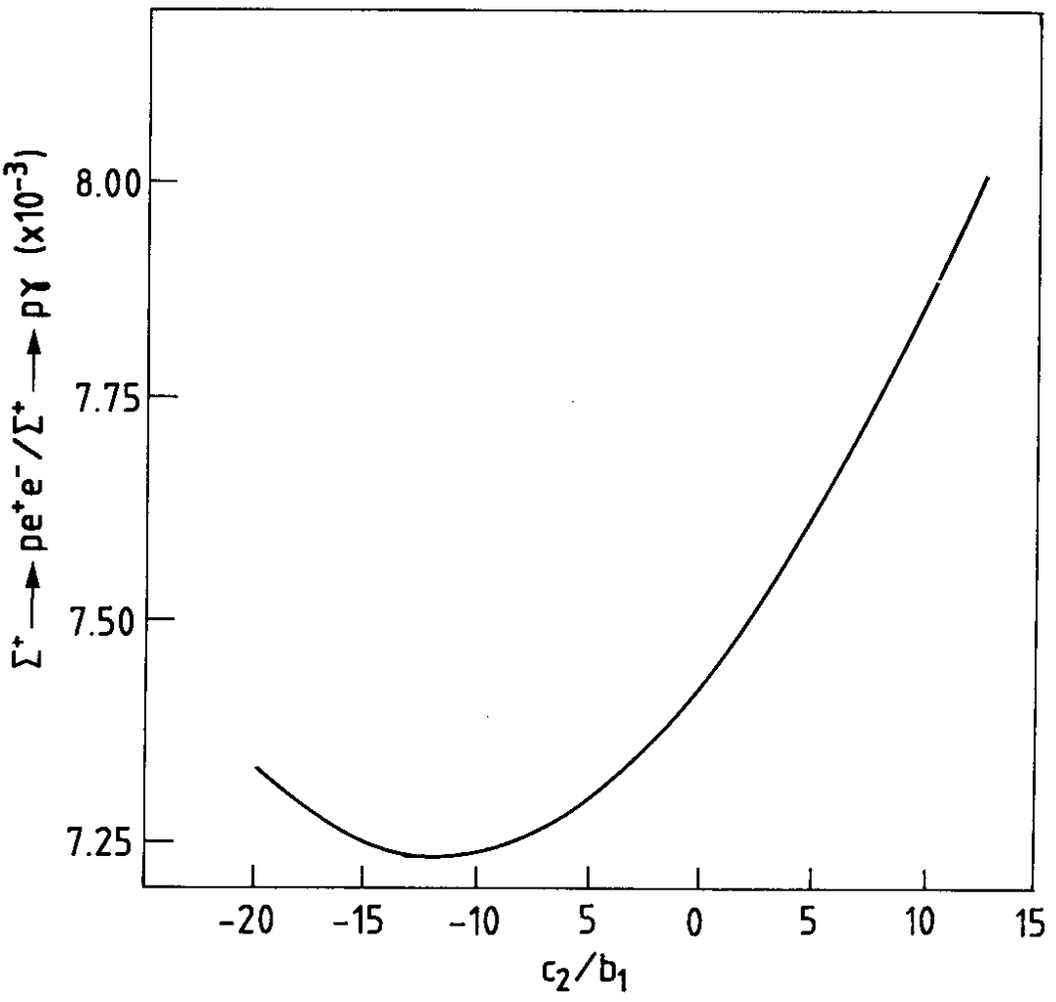
$\Sigma^+ \longrightarrow pe^+e^-/\Sigma^+ \longrightarrow p\gamma$ $(x10^{-3})$
8.00
7.75
7.50
7.25
-20
-15
-10
5
0
5
10
15
c_2/b_1

Fig. 5

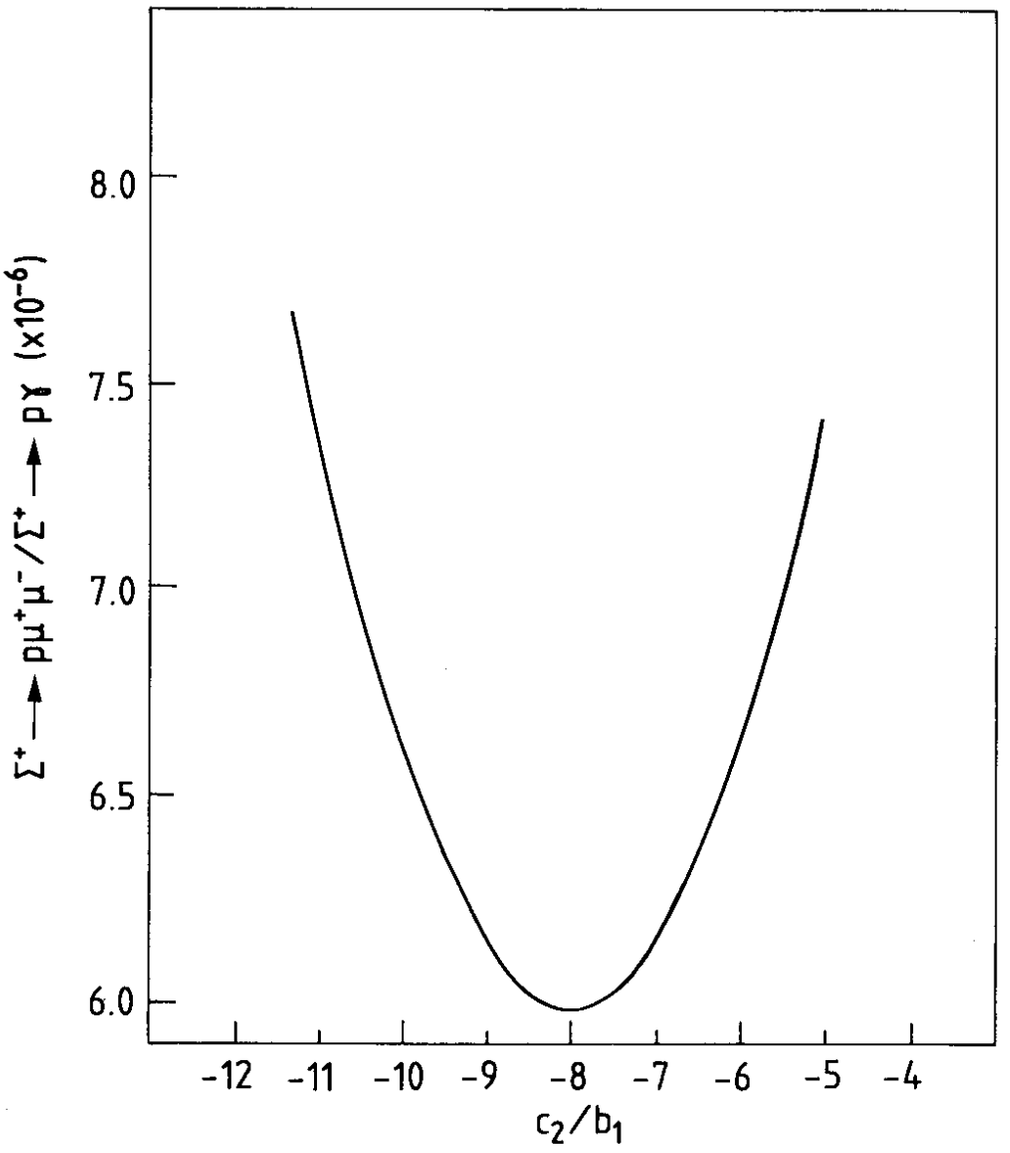
8.0
7.5
7.0
6.5
6.0
$\Sigma^+ \longrightarrow p\mu^+\mu^-/\Sigma^+ \longrightarrow p\gamma$ (x10^{-6})
-12
-11
-10
-9
-8
-7
-6
-5
-4
c_2/b_1

Fig. 6

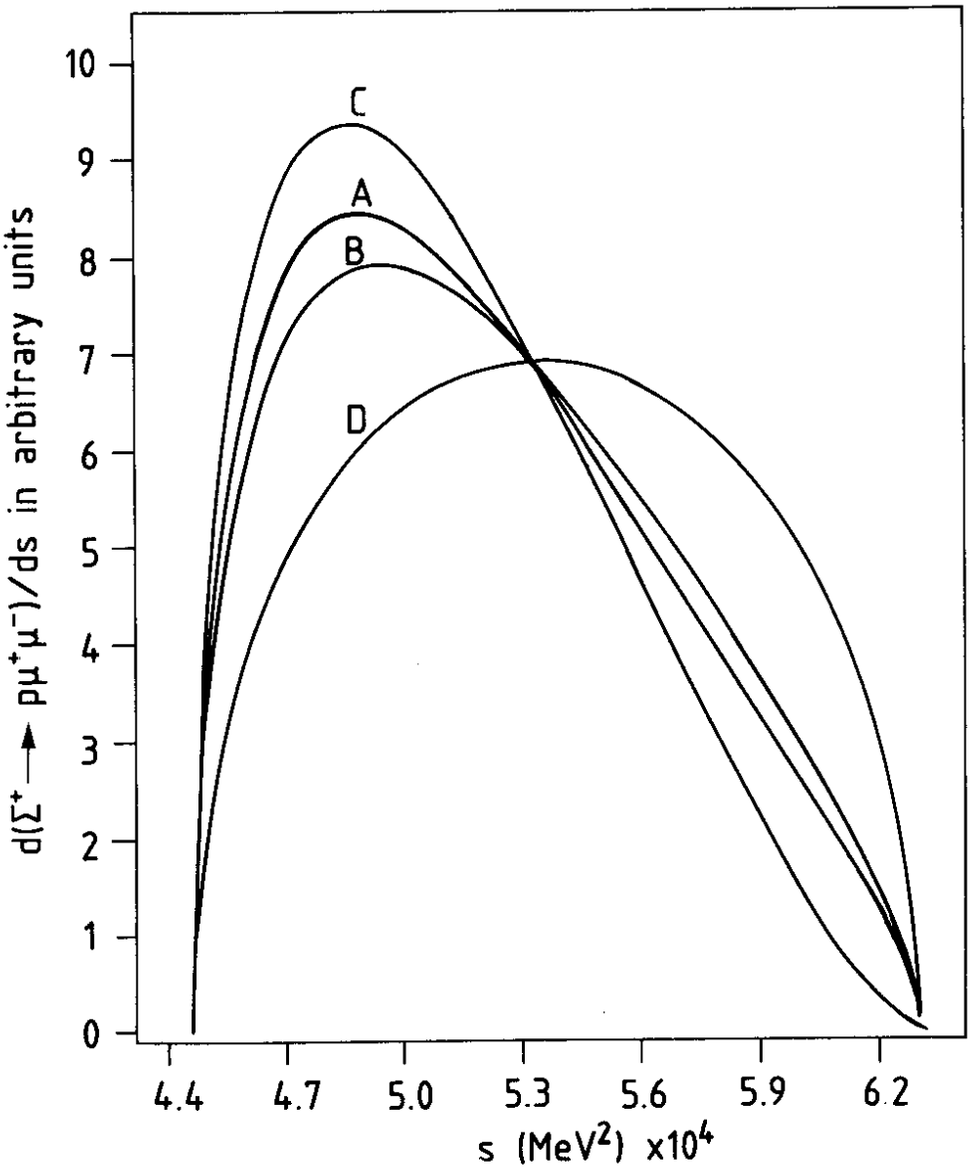
C
A
B
D
10
9
8
7
6
5
4
3
2
1
0
4.4
4.7
5.0
5.3
5.6
5.9
6.2
s (MeV²) x10⁴
d(Σ⁺ → pμ⁺μ⁻)/ds in arbitrary units

Fig. 7

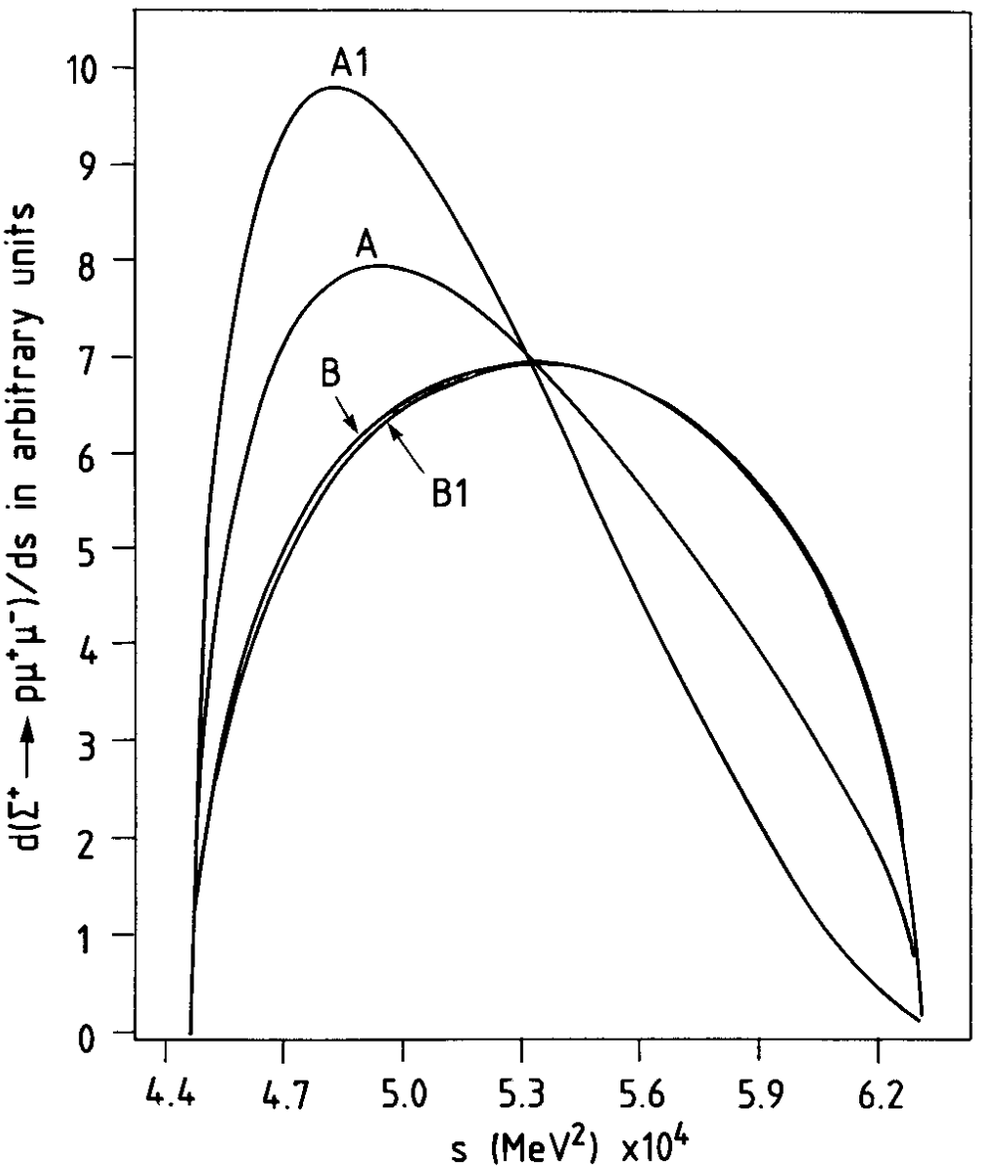
A1
A
B
B1
10
9
8
7
6
5
4
3
2
1
0
4.4
4.7
5.0
5.3
5.6
5.9
6.2
s (MeV²) x10⁴
d(Σ⁺ → pμ⁺μ⁻)/ds in arbitrary units

Fig. 8

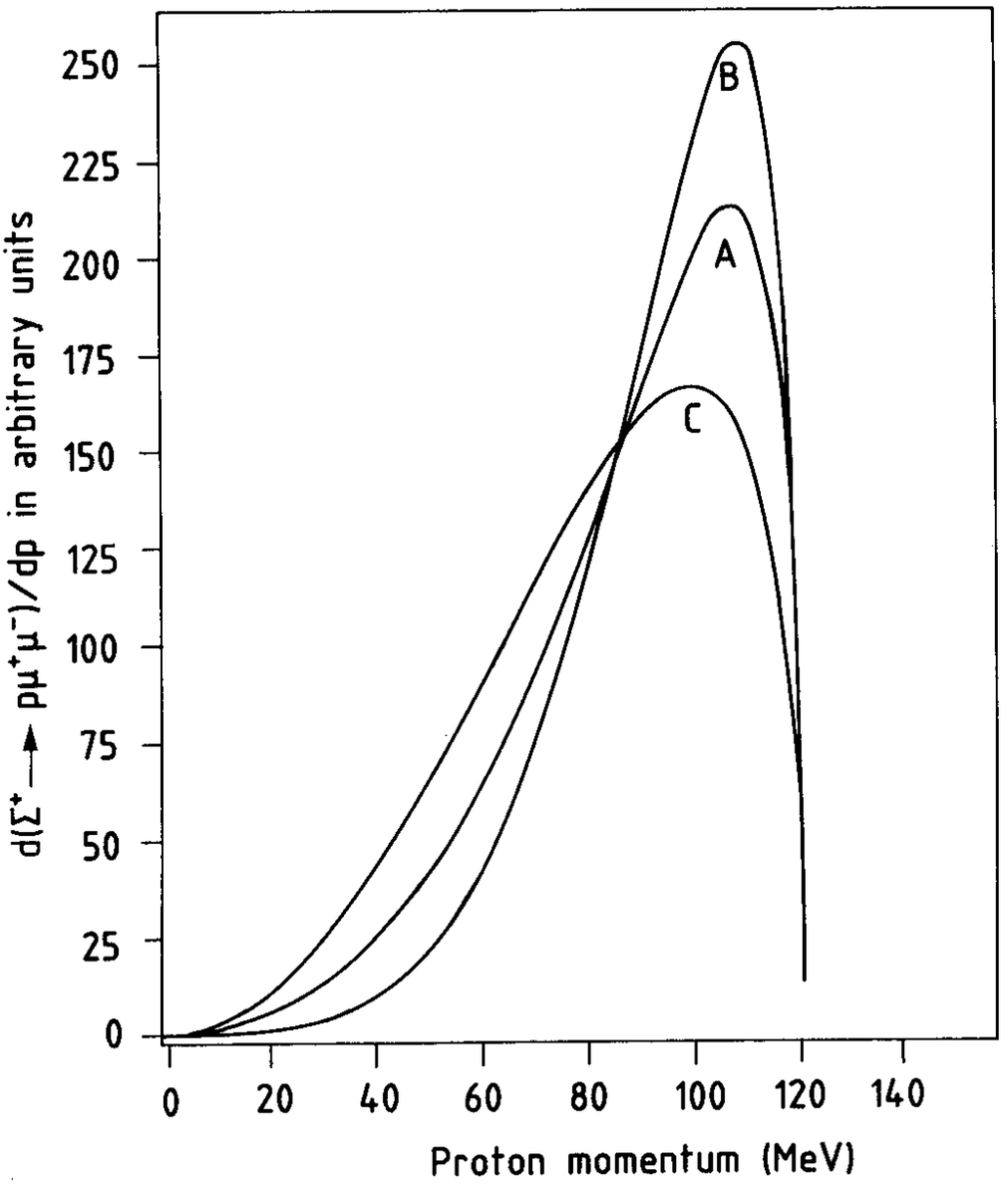
250
225
200
175
150
125
100
75
50
25
0
0
20
40
60
80
100
120
140
B
A
C
d(Σ⁺ → pμ⁺μ⁻)/dp in arbitrary units
Proton momentum (MeV)

Fig. 9

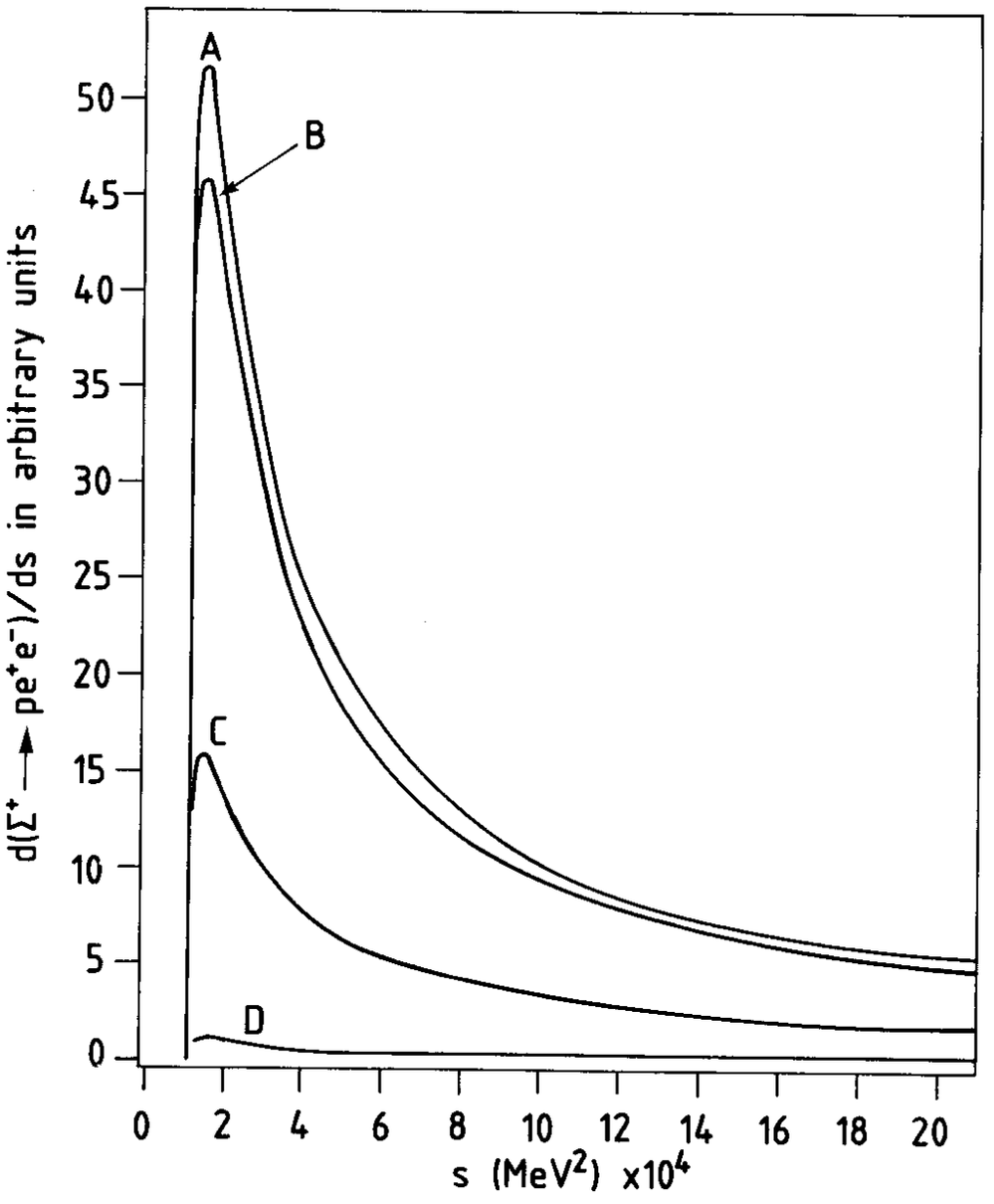
A
B
C
D
50
45
40
35
30
25
20
15
10
5
0
0
2
4
6
8
10
12
14
16
18
20
s (MeV²) x10⁴
d(Σ⁺ → pe⁺e⁻)/ds in arbitrary units

Fig. 10

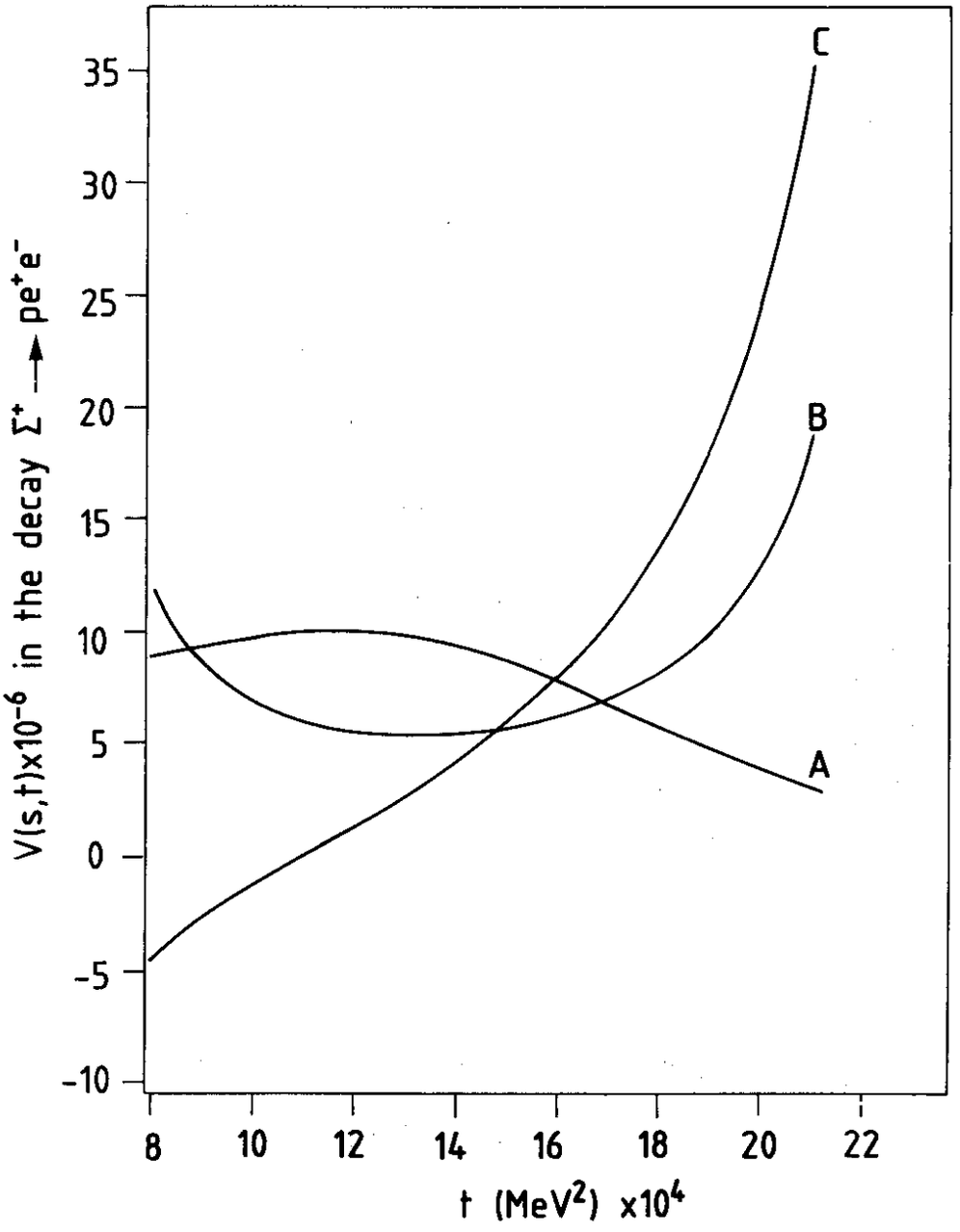
C
B
A
35
30
25
20
15
10
5
0
-5
-10
8
10
12
14
16
18
20
22
V(s,t)x10⁻⁶ in the decay Σ⁺ → pe⁺e⁻
t (MeV²) x10⁴

Fig. 11

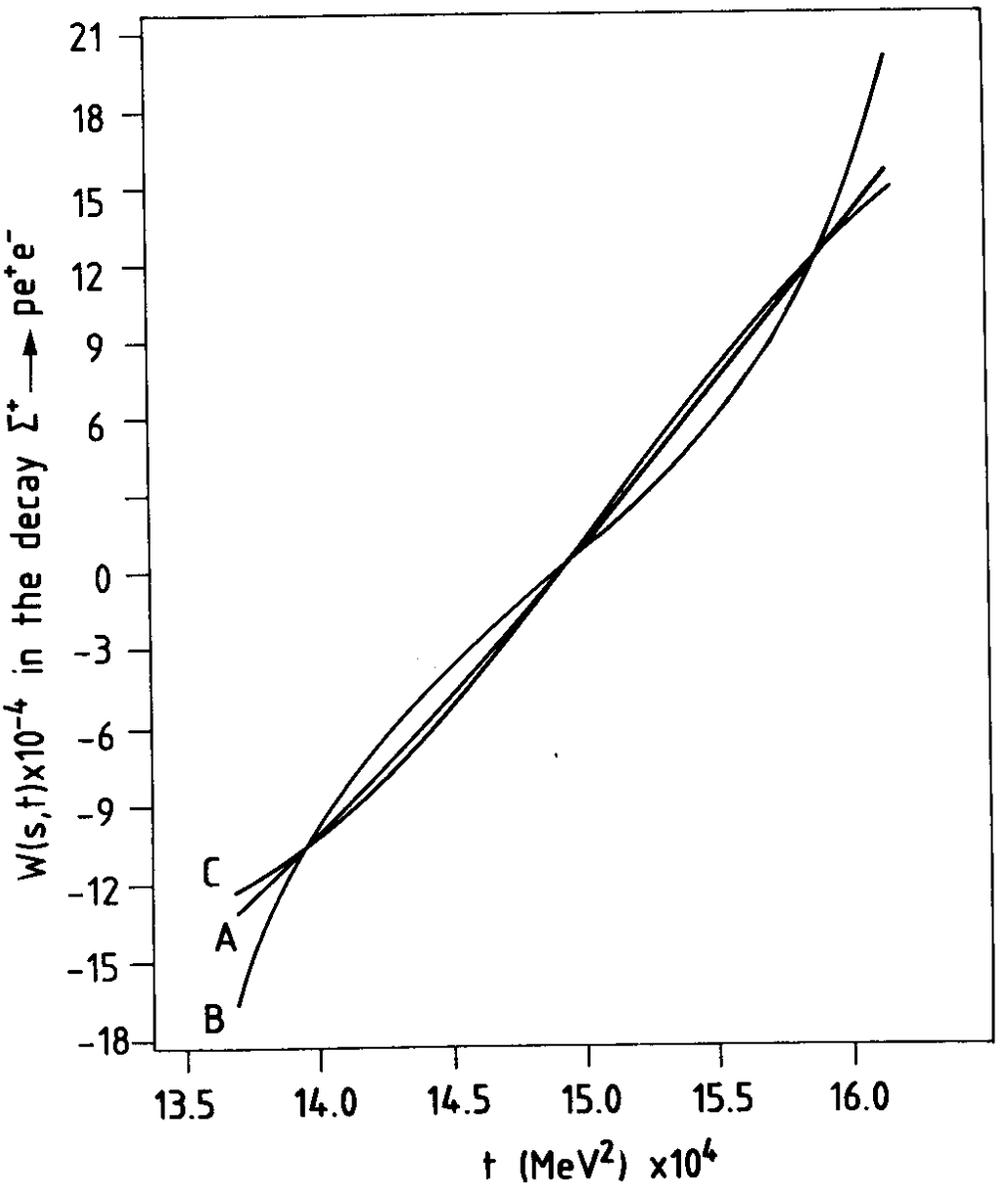
21
18
15
12
9
6
0
-3
-6
-9
-12
-15
-18
W(s,t)x10⁻⁴ in the decay Σ⁺ → pe⁺e⁻
C
A
B
13.5
14.0
14.5
15.0
15.5
16.0
t (MeV²) x10⁴

Fig. 12

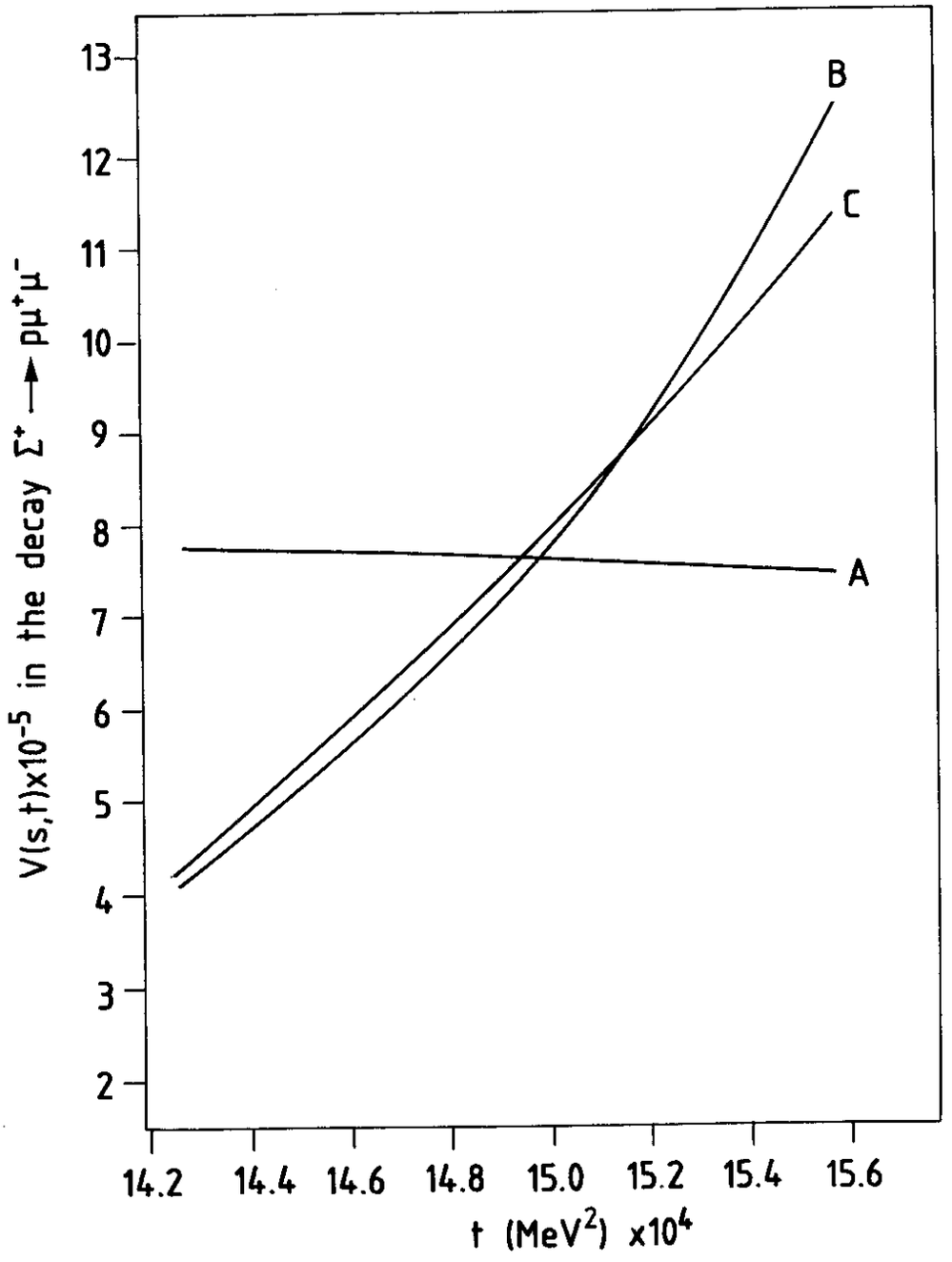
V(s,t)x10^{-5} in the decay $\Sigma^+ \rightarrow p\mu^+\mu^-$
13
12
11
10
9
8
7
6
5
4
3
2
B
C
A
14.2
14.4
14.6
14.8
15.0
15.2
15.4
15.6
t (MeV^2) x10^4

Fig. 13

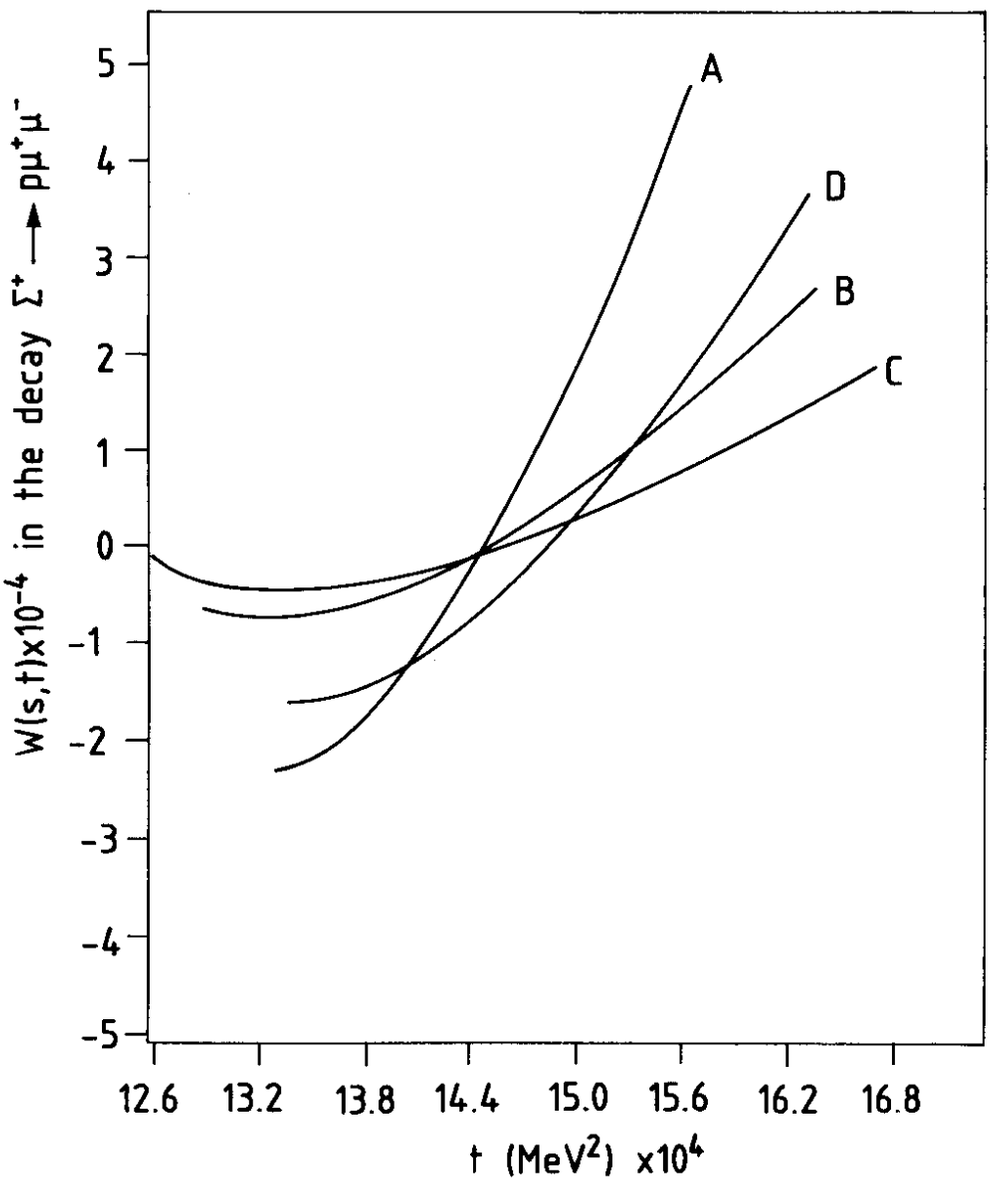
W(s,t)x10⁻⁴ in the decay Σ⁺ → pμ⁺μ⁻
5
4
3
2
1
0
-1
-2
-3
-4
-5
A
D
B
C
12.6
13.2
13.8
14.4
15.0
15.6
16.2
16.8
t (MeV²) x10⁴

Fig. 14

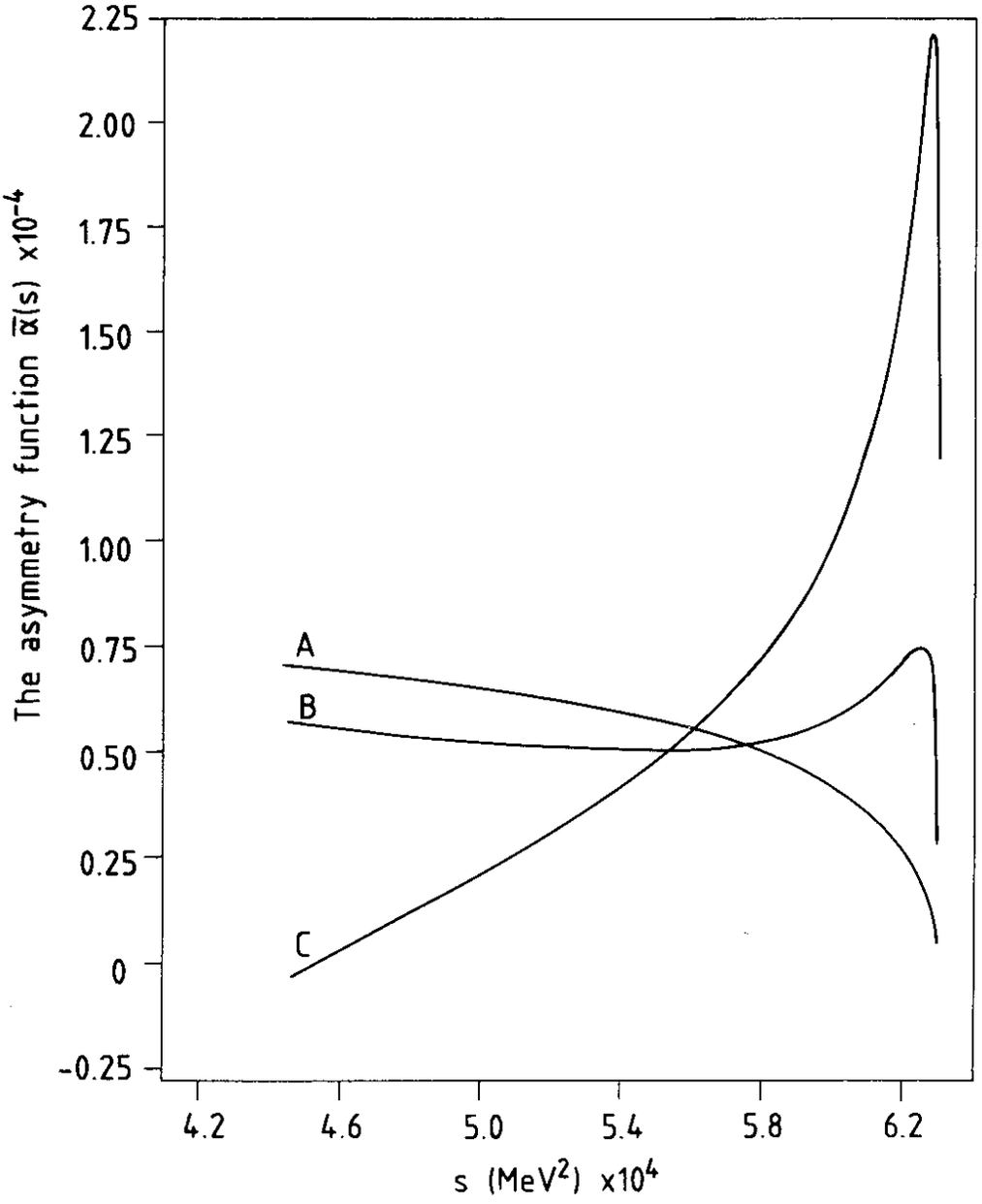
2.25
2.00
1.75
1.50
1.25
1.00
0.75
0.50
0.25
0
-0.25
The asymmetry function $\bar{\alpha}(s)$ x10^{-4}
A
B
C
4.2
4.6
5.0
5.4
5.8
6.2
s (MeV^2) x10^4

Fig. 15